University of Rhode Island

DigitalCommons@URI

2018

Identifications in Escape Regions of the Parameter Space of Cubic Polynomials

Chad Estabrooks
University of Rhode Island, estabrooksc@gmail.com

Recommended Citation

IDENTIFICATIONS IN ESCAPE REGIONS OF THE PARAMETER SPACE

OF CUBIC POLYNOMIALS

BY

CHAD ESTABROOKS

A DISSERTATION SUBMITTED IN PARTIAL FULFILLMENT OF THE

REQUIREMENTS FOR THE DEGREE OF

DOCTOR OF PHILOSOPHY

IN

MATHEMATICS

UNIVERSITY OF RHODE ISLAND

2018

DOCTOR OF PHILOSOPHY DISSERTATION

OF

CHAD ESTABROOKS

APPROVED:

Dissertation Committee:

Major Professor   Araceli Bonifant

Thomas Sharland

Mark Comerford

G. Faye Boudreaux-Bartels

Nasser H. Zawia
DEAN OF THE GRADUATE SCHOOL

UNIVERSITY OF RHODE ISLAND

2018

ABSTRACT

We investigate a relationship between escape regions in slices of the parameter space of cubic polynomials. The focus of this work is to give a precise description of how to obtain a topological model for the boundary of an escape region in the slice consisting of all cubic polynomials with a marked critical point belonging to a two cycle. To obtain this model, we start with the unique escape region in the slice consisting of all maps with a fixed marked critical point, and make identifications which are described using the identifications which are made in the lamination of the basilica map $z \mapsto z^2 - 1$.

ACKNOWLEDGMENTS

DEDICATION

This work is dedicated to my amazing wife, Sara. Her love and support has been essential to keeping me focused and grounded. She has cheerfully and heroically made great sacrifices in order for me to be able to pursue my education.

TABLE OF CONTENTS

LIST OF FIGURES

CHAPTER 1

Introduction

One of the major areas of holomorphic dynamics is the study of the iteration of holomorphic maps on the Riemann sphere $\widehat{\mathbb{C}} = \mathbb{C} \cup \{\infty\}$. It is well known that any holomorphic map of the sphere can be expressed as a rational function. Polynomials are also widely studied as a special case of the study of rational maps. The field began in the 1920's with two French mathematicians, Pierre Fatou and Gaston Julia. They showed that given a rational map, the Riemann sphere can be split into two disjoint sets. These sets came to be known as the Fatou set, where the dynamics are tame, and the Julia set, where the dynamics are chaotic. After this period of work, the subject was largely forgotten until the 1980's when Adrien Douady and John Hubbard proved many important results, see [1]. This resurgence of interest was due at least partially to having computers which could draw the complicated fractal images which arise from the iteration of holomorphic maps.

In studying quadratic polynomials, it is often helpful to consider those of the form $p_c(z) = z^2 + c$. We do not lose any information by doing so, since every quadratic polynomial is equivalent under a conformal change of variables to a unique polynomial of this form. In this way, we may study the parameter space of quadratic polynomials in one complex dimension using the single parameter $c \in \mathbb{C}$, see Figure 1. Given a parameter c, and a complex number z, we are interested in understanding the orbit of z under p_c, that is, the set $\{p_c^n(z) | n \in \mathbb{N}\}$, where p_c^n represents the n-times composition of the map p_c.

The study of cubic polynomials is more difficult, and far less is currently known than for quadratics. In polynomial dynamics, the orbits of critical points play an
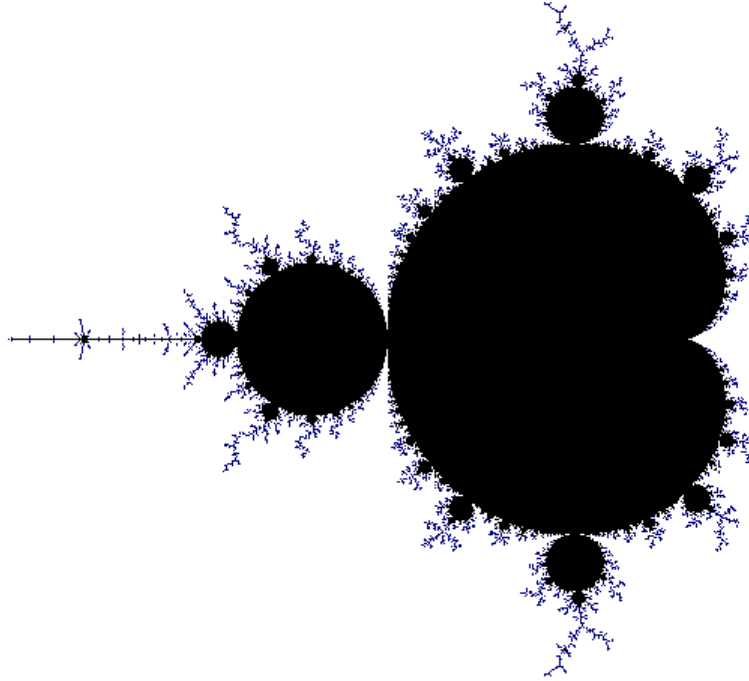
Figure 1. An image in the parameter space of quadratic polynomials, known as the Mandelbrot set.

essential role. Quadratic polynomials have only one critical point for which we need to keep track of the orbit. Cubics, on the other hand, have two. Not only does this mean that there is an extra critical orbit, but the orbits of the two critical points may interact, which creates new dynamical behavior not present in the quadratic case. Also, the parameter space of cubic polynomials is a two complex, or four real dimensional space. As a result, it is difficult to visualize. Therefore, as a way of studying this space, it is beneficial to slice it into one complex dimensional "cross sections," some of which will be studied in this work.

John Milnor came up with a very helpful way of defining these cross sections, see [2]. He started by considering the parameter space of cubic polynomials using the normal form $P_{a,v}(z) = z^3 - 3a^2z + (2a^3 + v)$. For a polynomial of this form, the critical points are at a and $-a$. As with quadratics, every cubic polynomial is
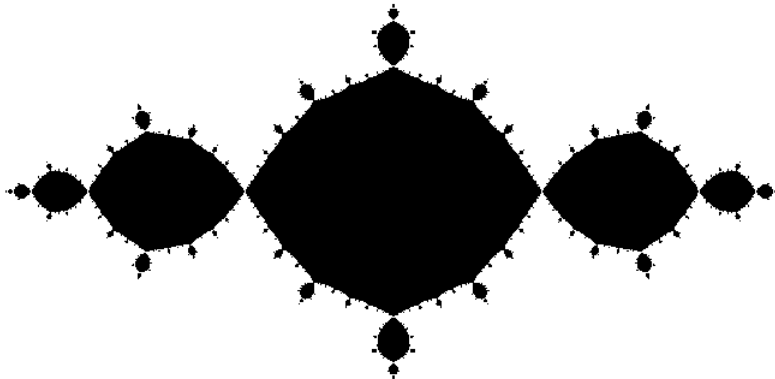
Figure 2. A well known quadratic Julia set known as the Basilica, corresponding to the map $z \mapsto z^2 - 1$.

conformally conjugate to a unique polynomial of this form. He then defined, for each natural number n, the curve $\mathcal{S}_n$ as the space consisting of all of the maps $P_{a,v}$ for which the critical point a has period exactly n. Fixing the behavior of the critical point a then simplifies our study, allowing us to look at the orbit of $-a$, and how it interacts with the known periodic orbit of a.

Each of these curves may be partitioned into two pieces. One of these pieces will be called the connectedness locus, $\mathcal{C}(\mathcal{S}_n)$, where the orbit of the free critical point remains bounded. This results in a Julia set which is connected. The other is called the escape locus, $\mathcal{E}(\mathcal{S}_n)$, where the orbit of the free critical point escapes to infinity. Julia sets for maps in the escape locus are disconnected. The escape locus of $\mathcal{S}_n$ can be divided into connected components, each of which is called an escape region, see [3]. The subset of hyberbolic maps (those for which the orbit of every critical point converges to an attracting cycle) in the connectedness locus consists of four types of components, depending on the interaction between the critical

3

orbits. In what is referred to as a type A component, both critical points lie in the same Fatou component (connected component of the Fatou set). In a type B component, $-a$ lies in a different Fatou component belonging to the same periodic cycle as that of a. In a type C component, the Fatou component containing $-a$ eventually maps into the periodic cycle of Fatou components of a. Finally, in a type D component, the cycles of Fatou components for each of the critical points are disjoint. John Milnor came up with the helpful terms adjacent, bitransitive, capture, and disjoint to aid in remembering the interaction between the critical points in type A,B,C, and D components, respectively.
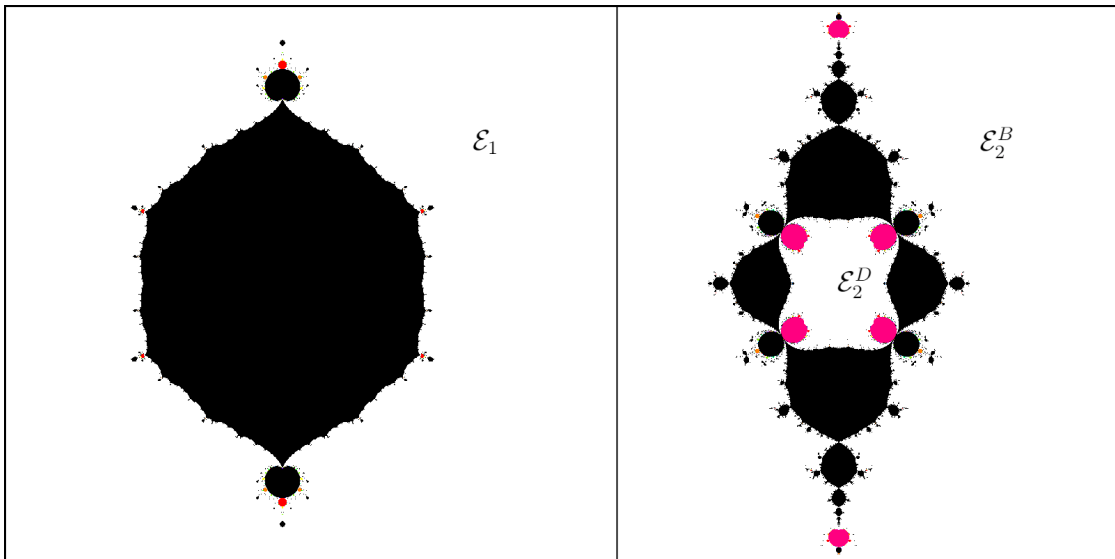
Figure 3. Connectedness loci of the curves $\mathcal{S}_1$ and $\mathcal{S}_2$ (left and right, respectively) shown side by side.

The parameter space of cubic polynomials has been studied by Matthieu Arfeux, Araceli Bonifant, Bodil Branner, John Hubbard, Hiroyuki Inou, John Milnor, and Pascal Roesch, among others. This work will focus on the escape regions of $\mathcal{S}_1$ and $\mathcal{S}_2$. As shown in Figure 3, in $\mathcal{S}_1$ there is a unique escape region, denoted $\mathcal{E}_1$, while in $\mathcal{S}_2$ there are two: $\mathcal{E}_2^D$, where the non-trivial connected components of the filled Julia sets resemble discs, and $\mathcal{E}_2^B$, where they resemble the basilica pictured

above in Figure 2, see [3]. We aim to give a precise description of a topological relationship between the boundaries of the escape regions $\mathcal{E}_1$ and $\mathcal{E}_2^B$.

Chapter 2 will present much of the background information necessary to the work, as well as develop a large portion of the notation to be used in the later chapters. A significant amount of time is spent here discussing various types of rays. We will discuss dynamic and parameter rays, and in each of these settings, both internal and external rays. Capital letters will be used in the notation of parameter rays, with lower case used in the case of dynamic rays. Subscripts will then be used to differentiate between internal and external rays. All four types of rays will be used frequently in obtaining the main results.

Chapter 3 will be a discussion of some known results in polynomial dynamics, with a focus on the basilica map which plays an essential role in the main results of this work. This chapter begins with the notion of a Hubbard tree, which is a topological tree associated with a polynomial p from which we can extract a surprising amount of dynamical information for p. Laminations are then discussed. The lamination of a polynomial p is an equivalence relation on $\mathbb{R}/\mathbb{Z}$, viewed as the boundary of a disc, which provides a topological model of the filled Julia set of p by considering the quotient of this closed disc by this equivalence relation. It is established that in the lamination of the basilica, any argument t with nontrivial equivalence class has a unique partner $\tilde{t} \neq t$. Such t will be referred to as a basilica angle with partner $\tilde{t}$, and the pair $\{t, \tilde{t}\}$ will be referred to as a basilica pair. The chapter is concluded with a brief discussion of hybrid equivalence, which will require the notion of a polynomial-like mapping.

Chapter 4 provides the details and development of the main results, which are presented in the results numbered 4.16 through 4.19. We will give here a brief summary of the findings. Consider the boundary of the unique escape region

$\partial \mathcal{E}_1 \subset \mathcal{S}_1$. Our main objective is to give a precise description of how to obtain a topological model for the boundary $\partial \mathcal{E}_2^B \subset \mathcal{S}_2$ of the basilica escape region from $\partial \mathcal{E}_1$. In Theorem 4.16, we consider first a single type C component of $\mathcal{S}_1$. Such a component is necessarily a topological disc, and we are therefore able to parametrize its boundary by the argument $t \in \mathbb{R}/\mathbb{Z}$ of the internal parameter ray in this component landing at each point. We then consider the equivalence relation from the lamination of the basilica map on this boundary, and the quotient by this relation provides our topological model for the components in $\mathcal{S}_2$ corresponding to this type C component in $\mathcal{S}_1$.

In $\mathcal{S}_1$ there is a unique type A component, referred to as the principal hyperbolic component, which we will denote $\widehat{\mathcal{H}}_0$. We obtain a similar result here, however there is an extra complication. The boundary of this component is also a topological circle, however we have a two-fold covering map from $\partial \widehat{\mathcal{H}}_0$ to $\mathbb{R}/\mathbb{Z}$ when associating each point on the boundary with the argument of the internal ray landing there. We then divide $\widehat{\mathcal{H}}_0$ into four quadrants, bounded by important internal rays, and proceed to define an equivalence relation. In Lemma 4.17, it is established that an identification will occur on the boundary of $\widehat{\mathcal{H}}_0$ at any landing map F of an internal ray whose argument is a basilica angle t with partner $\tilde{t}$, except when $t \in \left\{ \frac{1}{3}, \frac{2}{3} \right\}$. There are two possibilities for the map which is identified with F, namely the landing maps of each of the two internal rays of argument $\tilde{t}$. It is then established in Theorem 4.18 that it is the unique landing map of the ray of argument $\tilde{t}$ in the same quadrant of $\widehat{\mathcal{H}}_0$ as F which is identified with F. In Theorem 4.19, it is shown that there are no identifications at the landing maps of the four internal rays in $\widehat{\mathcal{H}}_0$ of arguments $\frac{1}{3}$ and $\frac{2}{3}$.

List of References

[1] A. Douady and J. H. Hubbard, "The Orsay notes," Available at www.picard. ups-tlse.fr/~buff/OrsayNotes/OrsayNotes.pdf.

[2] J. Milnor, "Cubic polynomial maps with periodic critical orbit, Part I," in *Complex Dynamics Families and Friends*, 2009, pp. 333–411.

[3] A. Bonifant, J. Kiwi, and J. Milnor, "Cubic polynomial maps with periodic critical orbit, Part II," *Conform. Geom. Dyn.*, vol. 14, pp. 68–112, 2010.

CHAPTER 2

Preliminaries

We begin our work on a topological relationship between boundaries of escape regions in slices of the parameter space of cubic polynomials with a discussion of the well known results necessary to the work. We will also set up much of the notation used throughout the work here.

2.1 Dynamical Systems and Conjugacy

We begin with the basics of general dynamical systems.

Definition 2.1. *A **dynamical system** is a pair (f, X) where X is a set, and*

$$f : X \to X$$

is a map.

Often the set X will have some type of structure, and the map f will preserve this structure. For example, X may be a topological or a measure space, then f would be a continous or measurable function, respectively. We are interested in studying the repeated application, or iteration, of the map f. We will use the notation

$$f^n = \underbrace{f \circ f \circ \ldots \circ f}_{n\text{-times}}$$

for the n-th iterate of f.

Definition 2.2. *Let (f, X) be a dynamical system, and $x \in X$. The **forward orbit** of x is the set $\{f^n(x)| \ n \in \mathbb{N}\}$.*

One goal of the study of dynamical systems is to understand as much as possible about the eventual tendencies of all forward orbits. Therefore, points with the simplest forward orbits play an important role.

Definition 2.3. *Let (f, X) be a dynamical system, and $x \in X$. The point x is* ***periodic of period n*** *if $f^n(x) = x$ and $f^i(x) \neq x$ for all $i \in \{1, ..., n-1\}$. A periodic point of period 1 is called a* ***fixed point*** *of f.*

Given two dynamical systems (f, X) and (g, Y), we have the following way of determining whether they are equivalent.

Definition 2.4. *Let (f, X) and (g, Y) be two topological dynamical systems. A* ***topological conjugacy*** *is a homeomorphism $\varphi : X \to Y$ satisfying*

$$\varphi \circ f \circ \varphi^{-1} = g.$$

Further, if (f, X) and (g, Y) are both conformal dynamical systems, by a conformal conjugacy, we will mean a conformal isomorphism $\varphi : X \to Y$ which satisfies the same composition property as given above. It can be helpful to view a conjugacy with a commutative diagram.

$$
\begin{array}{ccc}
X & \xrightarrow{\ f\ } & X \\
\downarrow{\scriptstyle\varphi} & & \downarrow{\scriptstyle\varphi} \\
Y & \xrightarrow{\ g\ } & Y
\end{array}
$$

If such a conjugacy exists, the orbits of the map are necessarily preserved in this diagram, and this gives us a way of comparing the dynamical systems.

2.2 Periodic Points and the Multiplier

Consider a polynomial p on $\widehat{\mathbb{C}}$. Given a fixed point $z_0 \in \mathbb{C}$ of p, we define the multiplier of p at z_0 as

$$\lambda_{z_0} = p'(z_0) \in \mathbb{C}.$$

We then classify the fixed point according to the size of its multiplier in the following way:

- $\lambda_{z_0} = 0$: z_0 is *superattracting*

- $|\lambda_{z_0}| < 1$: z_0 is *attracting*

- $|\lambda_{z_0}| > 1$: z_0 is *repelling*

- $|\lambda_{z_0}| = 1$: z_0 is *neutral* or *indifferent*

In the case of a periodic point z_0 of period n for p, we define the multiplier

$$\lambda_{z_0} = (p^n)'(z_0).$$

We then classify the periodic orbit in exactly the same way we classified fixed points above, by the size of this multiplier. For example, when $p^n(z_0) = z_0$ with n minimal and $|\lambda_{z_0}| < 1$, we say z_0 belongs to an attracting orbit of period n, or attracting n-cycle, for p.

Definition 2.5. *Let p be a polynomial with a periodic point z which is either attracting or superattracting (i.e. $0 \leq |\lambda| < 1$). The **basin of attraction** of z, denoted $\mathcal{A}_z$, is the open subset of the Riemann sphere which consists of all points whose orbits converge to the orbit of z. Further, the **immediate basin of attraction** of z, denoted $\widehat{\mathcal{A}}_z$, is the connected component of $\mathcal{A}_z$ containing z.*

2.3   Dynamics of Rational Maps and Polynomials

Definition 2.6. *A family $\mathcal{F}$ of holomorphic functions on the Riemann sphere is called a **normal family** if every infinite sequence of functions $\{f_n\}_{n\in\mathbb{N}}$ from $\mathcal{F}$ contains a subsequence which converges locally uniformly to some limit function f.*

Note that this limit function f is necessarily holomorphic, and need not be a member of the family $\mathcal{F}$.

Given a polynomial $p : \widehat{\mathbb{C}} \to \widehat{\mathbb{C}}$ of degree $d \geq 2$, the largest domain for which the family of iterates

$$\{p^n | n \in \mathbb{N}\}$$

is normal is called the Fatou set of p, and its complement is called the Julia set. We will denote the Julia set of p by $J(p)$, or simply J when the map is clear, and the Fatou set by $\widehat{\mathbb{C}} \setminus J$. When referring to a Fatou component, we will mean a connected component of the Fatou set.

We will illustrate with the simple example of the polynomial $p(z) = z^2$, with one critical point at 0. Let $z = re^{i\theta} \in \mathbb{C}$. We observe that $p(z) = r^2 e^{2i\theta}$, and further $p^n(z) = r^{2^n} e^{2^n i\theta}$. It then follows that when $r < 1$, $\lim_{n \to \infty} p^n(z) = 0$. The critical point at 0 is a superattracting fixed point whose basin of attraction is the open unit disc. When $r > 1$, $\lim_{n \to \infty} p^n(z) = \infty$, so all points outside of the closed unit disc converge to ∞. For $r = 1$, we have $p(e^{i\theta}) = e^{2i\theta}$, so the dynamics of p are conjugate to that of the chaotic doubling map $\theta \mapsto 2\theta$ on $\mathbb{R}/\mathbb{Z}$. The Julia set, where the map exhibits chaotic behavior, is then the unit circle $\partial \mathbb{D} = J(p)$. The two Fatou components for this map are the basin of attraction of 0, and the complement of the closed unit disc. This map is a very unusual exception, in that the Julia set is smooth.
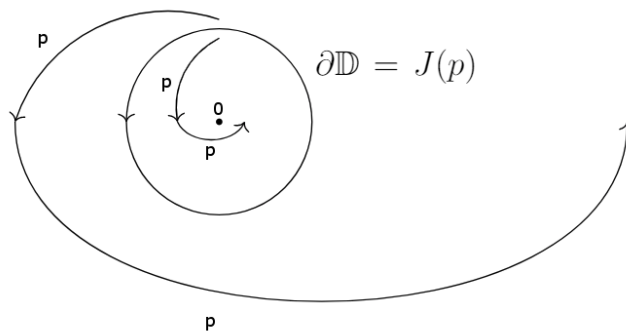
Figure 4. The dynamics of the map $z \mapsto z^2$.

In order to simplify our study of the dynamics of polynomial maps we will focus mainly on polynomials which are "centered." We have the following definition.

Definition 2.7. *A polynomial will be called **centered** if the sum of its critical points is zero.*

Quadratic polynomials have a single critical point in $\mathbb{C}$, so in order to be centered, this critical point must be at 0. Quadratics of the form $p(z) = z^2 + c$ satisfy this requirement. The centered cubic polynomials we will discuss take the form $F(z) = z^3 - 3a^2 z + (2a^3 + v)$. It is easily checked that the critical points of such polynomials are at a and $-a$, and these polynomials are therefore centered.

Definition 2.8. *Given a polynomial p, the **filled Julia set** of p, denoted $K(p)$, or simply K when the map is clear, is the set of all points $z \in \mathbb{C}$ which remain bounded under iteration of p.*

It is a result of Douady and Hubbard from [1] that the Julia set is the topological boundary of the filled Julia set, i.e. $J = \partial K$. We will need the following result from the same work.

Theorem 2.9 (Douady and Hubbard)**.** *The filled Julia set K of a polynomial p is topologically connected exactly when K contains all of the finite critical points of p.*

From the earlier example $p(z) = z^2$, $K(p)$ is the closed unit disc, which contains the critical point 0, and is connected.

In $\widehat{\mathbb{C}}$, it is clear that ∞ is fixed by any polynomial p. We define the multiplier at ∞ in general for a rational map, and comment on the special case for polynomials.

Definition 2.10. *Let R be a rational map for which ∞ is periodic of period n. The **multiplier at** ∞ is defined as $\lambda_\infty = \lim\limits_{z \to \infty} \frac{1}{(p^n)'(z)}$.*

Now, for a polynomial p of degree $d \geq 2$, we know that $p'(z)$ is a polynomial of degree $d - 1 \geq 1$, so that the multiplier λ_∞ is always 0, and hence ∞ is a superattracting fixed point.

Definition 2.11. *For a polynomial p of degree $d \geq 2$, the **basin of attraction of** ∞, denoted by $\mathcal{A}(\infty)$, is the complement of the filled Julia set, $\widehat{\mathbb{C}} \setminus K$. In other words, it is the open set consisting of all points whose orbits tend to ∞.*

This agrees with our previous definition of a basin of attraction. Further, due to the maximum modulus principle, the basin of attraction of ∞ corresponds exactly with the immediate basin as defined earlier.

Here we discuss another example, which will be of significant importance to this work. Consider

$$p(z) = z^2 - 1.$$

This polynomial is centered, as its one critical point is at zero. The critical point is periodic of period two, as $p(0) = -1$ and $p(-1) = 0$. Therefore, $0 \in K(p)$, and $K(p)$ is connected by Theorem 2.9. The filled Julia set of this quadratic polynomial is called the basilica, and is pictured in Figure 5.

2.4   Böttcher's Theorem and Rays

We will make use of the following theorem of Böttcher, from [2, Theorem 9.1], to make some constructions which will be essential to our work. The local degree of a holomorphic function f about a point $z \in \widehat{\mathbb{C}}$ is the number of preimages under f, counted with multiplicity, of any point in a sufficiently small neighborhood of the point z.

Theorem 2.12 (Böttcher)**.** *Let $n \geq 2$, and suppose $f(z) = a_n z^n + a_{n+1} z^{n+1} + ...$ is a holomorphic function with a superattracting fixed point at 0, around which f has local degree n. Then there is a local holomorphic change of coordinate $w = \phi(z)$,*
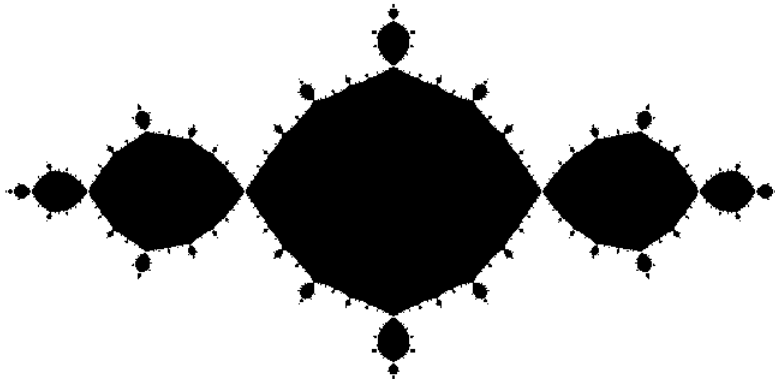
Figure 5. The filled Julia set of the map $z \mapsto z^2 - 1$, called the basilica.

with $\phi(0) = 0$, which conjugates f to the nth power map $w \mapsto w^n$ throughout some neighborhood of zero. Furthermore, ϕ is unique up to multiplication by an (n - 1)st root of unity.

Let p be a polynomial with a fixed simple critical point at z_0, for which the immediate basin $\widehat{\mathcal{A}}_{z_0}$ does not contain another critical point of p. Then we may apply Böttcher's theorem to get a map ϕ in some neighborhood of z_0. We then extend, pulling back by the dynamics of p. This expands the domain and range of ϕ. Since there are no other critical points in $\widehat{\mathcal{A}}_{z_0}$, we may extend so that this extension is defined on all of $\widehat{\mathcal{A}}_{z_0}$, and takes its values in the unit disc $\mathbb{D}$. This Böttcher coordinate conjugates p to the squaring map, since p has local degree two about a simple critical point. It also follows that this map is unique since the local degree is two.

Definition 2.13. *Let p and z_0 be as described above. Given $t \in \mathbb{R}/\mathbb{Z}$, the **internal ray of argument** t for $\widehat{\mathcal{A}}_{z_0}$ is*

$$r_i(t) := \phi^{-1}(\{re^{2\pi it}|0 < r < 1\}).$$

14

For such rays, $\lambda_i(t) := \lim\limits_{s \to 1^-} \phi^{-1}(se^{2\pi it}) \in \partial\widehat{\mathcal{A}}_{z_0}$ exists, and is referred to as the landing point of the ray.

When necessary to emphasize the map for any ray or landing point, we will use a superscript, i.e. in this case, $r_i^p(t)$ and $\lambda_i^p(t)$ will be the internal ray of argument t and its landing point for the polynomial p.

Notice that in this local degree two case, $p(r_i(t)) = r_i(2t)$. We may define internal rays in any other component of $\mathcal{A}_{z_0}$ by taking appropriate preimages of the rays in the immediate basin $\widehat{\mathcal{A}}_{z_0}$.

Consider a polynomial p of degree $d \geq 2$. From the discussion after Definition 2.10, this polynomial has a superattracting fixed point at ∞. From Böttcher's theorem, there is a maximal neighborhood V of ∞ and a corresponding minimal $r \geq 1$ such that we have the map

$$\phi : \widehat{\mathbb{C}} \setminus \overline{V} \to \widehat{\mathbb{C}} \setminus \overline{D_r},$$

with the property

$$\phi(p(z)) = \phi(z)^d.$$

Adding the requirement that $\lim\limits_{z \to \infty} \frac{\phi(z)}{z} = z$, in which case we say ϕ is tangent to the identity near ∞, there is a unique such map. When p is such that $K(p)$ is connected, it follows that we may choose $V = \mathcal{A}(\infty)$, and $r = 1$ since there are no critical points in $\mathcal{A}(\infty)$. In order to avoid unnecessary complexity, we will hold off on further discussion of the case of disconnected filled Julia set, and discuss later only a special case for certain cubic polynomials. We will refer to the map ϕ as the Böttcher coordinate, or Böttcher isomorphism of the polynomial p. When necessary, we will use the notation ϕ_p to emphasize the map.

Definition 2.14. *Let p be a polynomial with connected filled Julia set. For $t \in$*

15

$\mathbb{R}/\mathbb{Z}$, the **external ray of angle** t for p is defined as

$$r_e(t) := \{\phi^{-1}(re^{2\pi it})|r > 1\}.$$

We say that the ray $r_e(t)$ lands at $z \in J(p)$ if $z = \lim_{s \to 1^+} \phi^{-1}(se^{2\pi it})$ (in particular, the limit exists). We will denote the landing point by $\lambda_e(t)$.
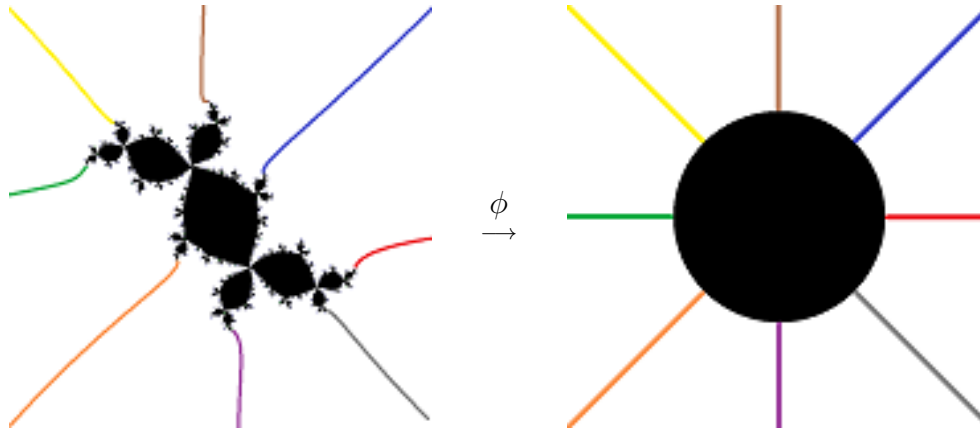
Figure 6. Rational external rays of denominator eight for a quadratic polynomial known as Douady's rabbit.

We have the following result, from [2, Theorem 17.14].

Theorem 2.15 (Carathéodory). *A conformal isomorphism $\psi : \mathbb{D} \to U \subset \widehat{\mathbb{C}}$ extends to a continuous map from the closed disk $\overline{\mathbb{D}}$ onto $\overline{U}$ if and only if the boundary ∂U is locally connected, or equivalently if and only if the complement $\widehat{\mathbb{C}} \setminus U$ is locally connected.*

Therefore, the map

$$\lambda_e : \mathbb{R}/\mathbb{Z} \to J(p)$$

sending each argument to the landing point of the corresponding ray is well defined whenever the Julia set is connected and locally connected. This map will be referred to as the Carathéodory loop.
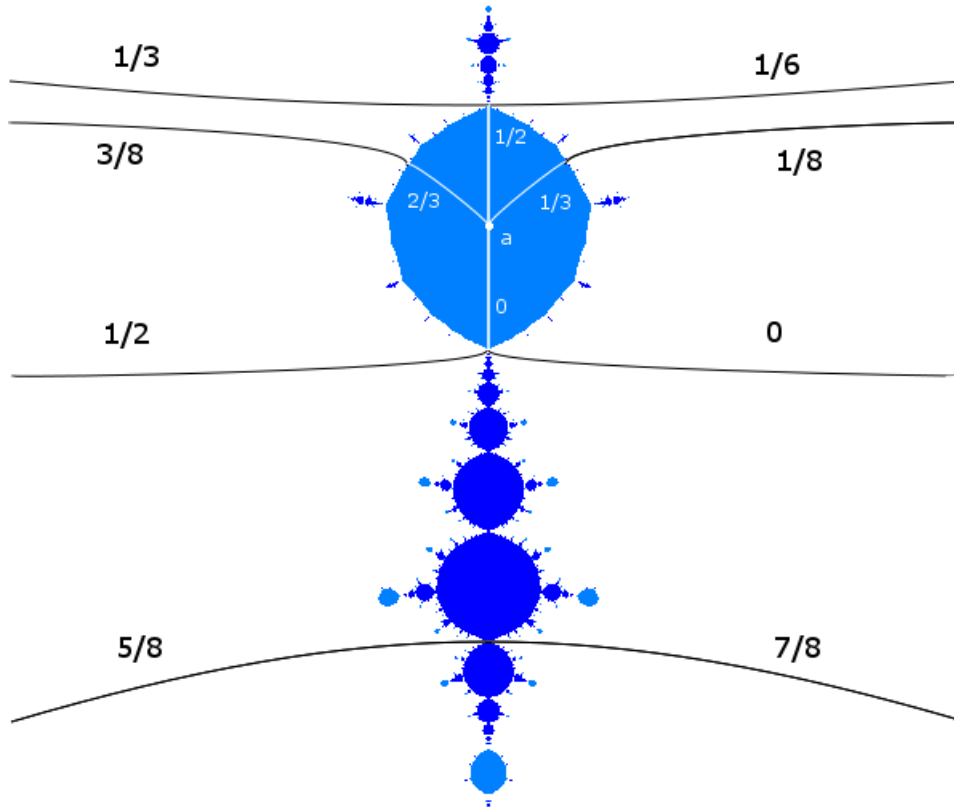
Figure 7. A cubic polynomial with superattracting fixed point at $a = 0.78i$, and some internal and external rays marked.

Definition 2.16. *For any polynomial p of degree $d \geq 2$, the **Green's function***

$$G_p : \mathbb{C} \to [0, \infty)$$

associated with p is defined as

$$G_p(z) = \begin{cases} \log |\phi_p(z)|, & z \in \mathbb{C} \setminus K(p) \\ 0, & z \in K(p) \end{cases}$$

where $\phi_p(z)$ is the Böttcher coordinate for p.

The Green's function is continuous, harmonic outside of $K(p)$, takes the value 0 on $K(p)$, and increases as the input travels along an external ray from $K(p)$ towards ∞.

Definition 2.17. *The level curve of the Green's function $\{z|G_p(z) = c\}$ will be referred to as the **equipotential** of height c.*

The equipotential of height c for a degree d polynomial is mapped under p onto the equipotential of height $c \cdot d$ by a d-fold covering.

2.5 Cubic Polynomials

We will now begin to focus our study on cubic polynomials. Every cubic polynomial is affinely conjugate to one which is monic and centered. We are interested in studying the parameter space. We may represent any monic and centered cubic polynomial in the Branner Hubbard normal form

$$p(z) = z^3 - 3a^2 z + b,$$

introduced in [3]. Using the coordinates (a, b) we may identify the parameter space of such polynomials, which we will denote by $\mathcal{P}(3)$, with $\mathbb{C}^2$.

Following John Milnor in [4], it will be convenient for us to consider monic and centered cubic polynomials with a marked critical point a having the associated critical value v. Such a polynomial takes the form

$$F(z) = z^3 - 3a^2 z + (2a^3 + v).$$

We will refer to the critical point at $-a$ as the free critical point, and refer often to the associated cocritical point $2a$, for which $F(-a) = F(2a)$. We may use the coordinates (a, v) to identify the space of such polynomials with $\mathbb{C}^2$. This parameter space we will denote by $\widehat{\mathcal{P}}(3)$, and we notice that it is a two fold covering of $\mathcal{P}(3)$, ramified at $a = v = 0$.

Definition 2.18. *The **connectedness locus** in $\widehat{\mathcal{P}}(3)$ will be defined to be the set of all maps in $\widehat{\mathcal{P}}(3)$ whose filled Julia set is connected. We will denote the connectedness locus by $\mathcal{C}(\widehat{\mathcal{P}}(3))$.*

Recall from Theorem 2.9, it follows that for a map belonging to the connectedness locus, the orbits of both critical points remain bounded. This connectedness locus is difficult to visualize and study since it lives in two complex dimensions. Therefore, John Milnor came up with a way of slicing it into one complex dimensional pieces which can then be viewed and studied.

2.6 Milnor's Curves in Cubic Parameter Space

The following definition is due to Milnor in [4].

Definition 2.19. *For $n \in \mathbb{N}$, the curve $\mathcal{S}_n$ in $\widehat{\mathcal{P}}(3)$ will be defined to be the set of all maps in $\widehat{\mathcal{P}}(3)$ for which the marked critical point a has period exactly n. Further, $\mathcal{C}(\mathcal{S}_n)$ will be used to denote the connectedness locus $\mathcal{C}(\widehat{\mathcal{P}}(3))$ intersected with the curve $\mathcal{S}_n$.*

Our focus will be on the curves $\mathcal{S}_1$ and $\mathcal{S}_2$, or more specifically, the boundaries of $\mathcal{C}(\mathcal{S}_1)$ and $\mathcal{C}(\mathcal{S}_2)$.

Suppose we have a map $F \in \mathcal{S}_1$. Then the marked critical point has period 1, or in other words, is a fixed point of F. Therefore, we have that $F(a) = v = a$, and Milnor gave a parameterization of this curve using the normal form

$$F(z) = z^3 - 3a^2 z + (2a^3 + a),$$

depending only on the one complex parameter a. This allows us to get a one complex dimensional picture of this curve, and its connectedness locus, see Figure 8.

Similarly for a map $F \in \mathcal{S}_2$, we will now require that the marked critical point belong to the period two orbit $a \mapsto v \mapsto a$. We define the displacement $\delta = v - a \in \mathbb{C}$, and after some algebra we arrive at the normal form

$$F(z) = z^3 - 3\left(-\frac{\delta + \frac{1}{\delta}}{3}\right)^2 z + \left(2\left(-\frac{\delta + \frac{1}{\delta}}{3}\right)^3 + \left(-\frac{\delta + \frac{1}{\delta}}{3}\right) + \delta\right),$$
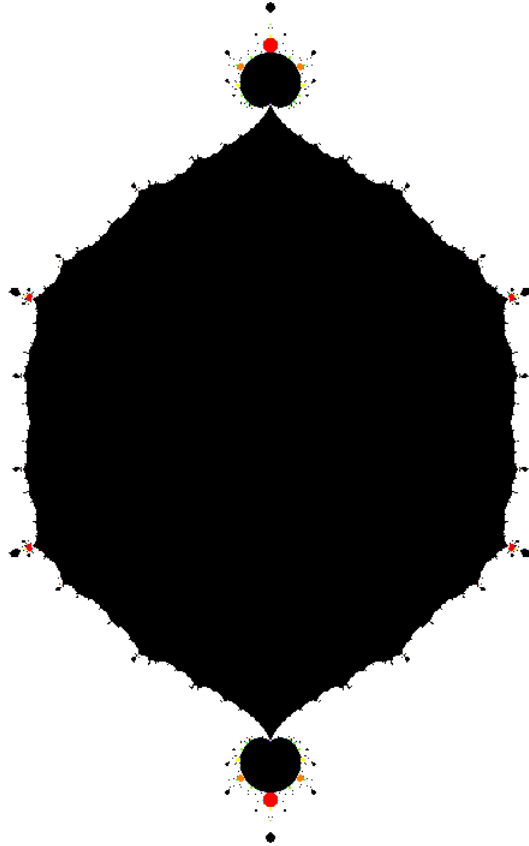
Figure 8. A projection into one complex dimension of the curve $\mathcal{S}_1$.

which can be used to parameterize the curve $\mathcal{S}_2$ with the single complex parameter δ. We now make the important simple observation that for a map in any curve $\mathcal{S}_n$, connectedness of the filled Julia set is equivalent to boundedness of the orbit of the free critical point $-a$. This is because the only other finite critical point belongs to a periodic orbit which is necessarily bounded.

We now turn our attention to the hyperbolic components of the curves $\mathcal{S}_n$.

Definition 2.20. *A map is called **hyperbolic** if the orbit of every critical point converges to an attracting cycle.*

The hyperbolic components of $\mathcal{S}_n$ are then the connected components of the
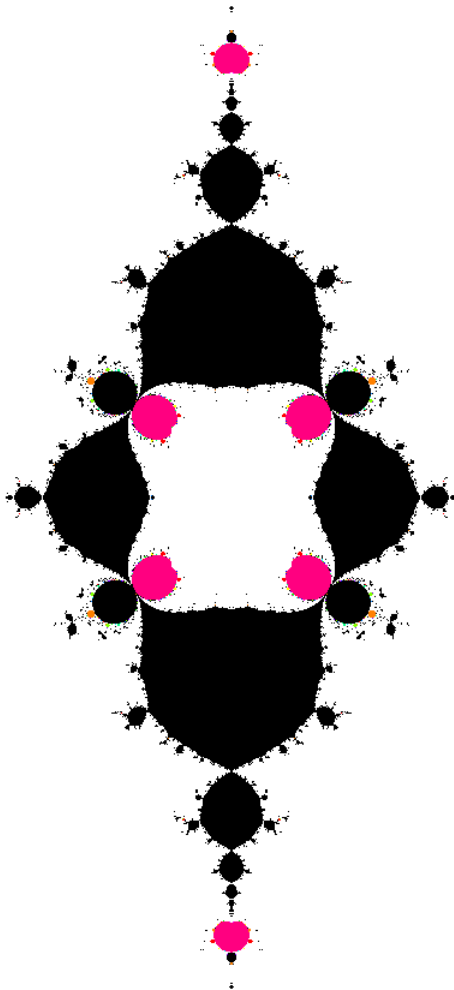
Figure 9. A projection into one complex dimension of the curve $\mathcal{S}_2$.

set of all hyperbolic maps in $\mathcal{S}_n$. We will first focus on the hyperbolic components contained in the connectedness locus $\mathcal{C}(\mathcal{S}_n)$. Milnor, using similar ideas to the work of Mary Rees on quadratic rational maps in [5], classified the hyperbolic components in $\mathcal{C}(\mathcal{S}_n)$ into the following four types, according to how the orbits of the two critical points interact with each other. Note that for a hyperbolic map, each critical point belongs to a Fatou component, and if the map is in the

connectedness locus, then the Fatou components containing the critical points are necessarily bounded Fatou components.

Type A: (Adjacent) Both critical points belong to the same Fatou component.

Type B: (Bitransitive) The two critical points belong to different Fatou components belonging to the same periodic cycle.

Type C: (Capture) The Fatou component of the free critical point joins the cycle of Fatou components of the marked critical point after some positive number of iterations.

Type D: (Disjoint) The cycles of Fatou components for the critical points never meet.

We observe that $\mathcal{C}(\mathcal{S}_n)$ contains hyperbolic components of all four types with one clear exception. The existence of a type B component requires that neither critical point in that component be fixed. By definition, this can not happen within $\mathcal{C}(\mathcal{S}_1)$.

While we may define rays for any hyperbolic component, they are all defined in a different way, and we will only require the definitions for type A and C components. We will begin with the simplest case of a type C component of $\mathcal{S}_1$. We know that for a map p in such a component, the cocritical point $2a_p$ is mapped eventually into the immediate basin of the marked critical point a_p. Let $n \in \mathbb{N}$ be minimal such that $p^n(2a_p) \in \widehat{\mathcal{A}}_{a_p}$.

Definition 2.21. *For a map p in a type C component of $\mathcal{S}_1$, there is a unique argument t such that $p^n(2a_p)$ lies on the dynamic ray $r_i(t)$ in $\widehat{\mathcal{A}}_{a_p}$. We then say that p lies on the **internal parameter ray** of argument t. We will denote this internal parameter ray by $R_i(t)$. When $R_i(t)$ lands, the landing map will be denoted $\Lambda_i(t)$.*
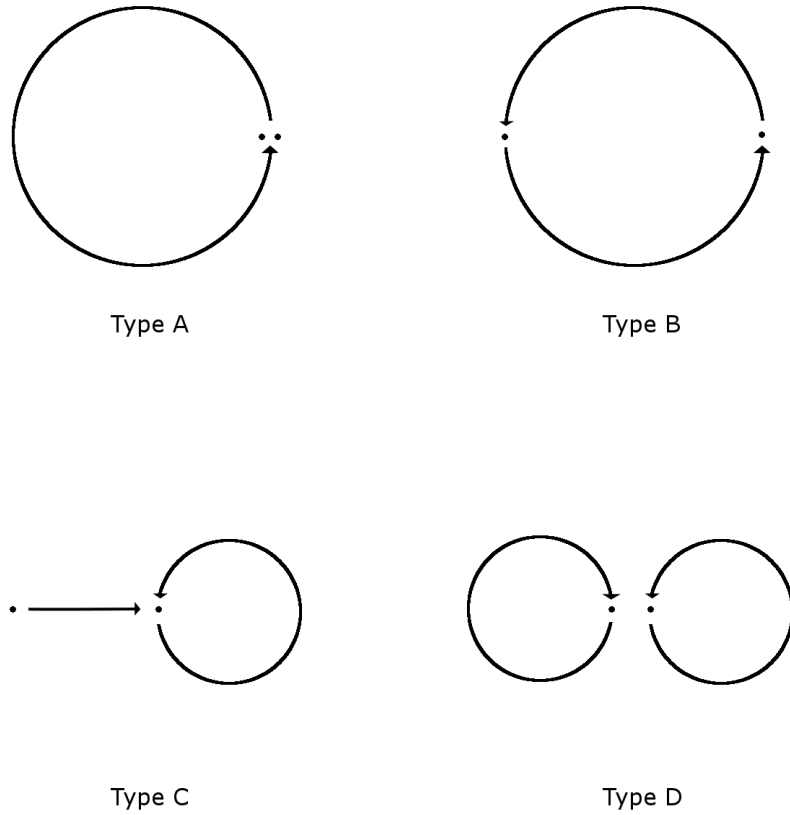
Figure 10. Illustrations which demonstrate the interactions between the two critical points in the four different types of components.

Since, by [6, Theorem 1], the boundary of every hyperbolic component of the connectedness locus $\mathcal{C}(\mathcal{S}_1)$ is a Jordan curve, hence locally connected; it follows from Theorem 2.15 that the landing point $\Lambda_i(t)$ always exists.

There is a unique type A component of $\mathcal{S}_1$ which we will call the principal hyperbolic component, and denote $\widehat{\mathcal{H}}_0$. We are interested in defining internal rays in $\widehat{\mathcal{H}}_0$ as well. In this case, the Böttcher coordinate can not be extended to the entire immediate basin of a, because of the presence of the free critical point $-a$. The Böttcher coordinate may be extended until the domain reaches $-a$. There is then an internal ray for which the landing point is $-a$.
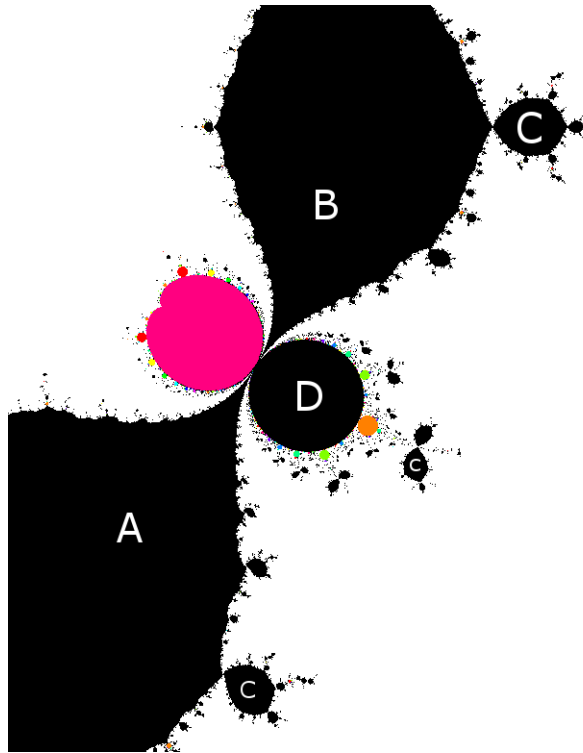
Figure 11. A piece of $\mathcal{C}(\mathcal{S}_2)$ with components of all four types labeled.

Definition 2.22. *Consider the set of maps $p \in \widehat{\mathcal{H}}_0$ for which the internal dynamic ray of argument t lands at $-a$. Each of the two connected components of this set will be referred to as an **internal parameter ray of argument t**, and denoted $R_i(t)$.*

We observe that as the parameter travels a loop around the center of $\widehat{\mathcal{H}}_0$, the free critical point makes two loops around the marked critical point in the dynamical plane. The map $a \mapsto t$ sending a parameter in $\widehat{\mathcal{H}}_0$ to its internal argument $t \in \mathbb{R}/\mathbb{Z}$ is then a two fold cover, ramified at $a = 0$. For more information, see [4, Section 3]. We will use the notation $\widehat{\Lambda}_i(t)$ to represent the set of the two landing maps for the internal rays of argument t.

2.7 Escape Regions

We now look at the subset of hyperbolic maps in $\mathcal{S}_n$ called the escape locus, which consists of all maps outside of the connectedness locus, as studied in [7]. The name comes from the fact that for such maps, the orbit of the free critical point "escapes" to ∞, and hence the filled Julia sets are disconnected. We will refer to the connected components of the escape locus as escape regions. There is a unique escape region in $\mathcal{S}_1$, which we will denote by $\mathcal{E}_1$. In $\mathcal{S}_2$, the escape locus consists of two escape regions, which we will distinguish by the connected components of the filled Julia sets, see [7]. We will also provide further details on this in Chapter 3. There is an escape region of $\mathcal{S}_2$ where each nontrivial connected component of the filled Julia set is homeomorphic to a disc, which will be denoted $\mathcal{E}_2^D$. In the other, each nontrivial component is homeomorphic to the basilica. This region will be denoted $\mathcal{E}_2^B$. For maps in these regions, we will refer to a main component K_a of K, which contains the marked critical point a. For maps in $\mathcal{E}_1$ and $\mathcal{E}_2^B$, these main components are forward invariant, and all other nontrivial components of K are eventually mapped onto the main component.

We now want to consider dynamic rays for the maps in escape regions of $\mathcal{S}_1$ and $\mathcal{S}_2$, whose filled Julia sets are disconnected. Consider such a polynomial p. As before, there is a Böttcher coordinate ϕ defined in a neighborhood of ∞, which conjugates p to $z \mapsto z^3$ since a cubic polynomial has local degree three near ∞. Similarly to our previous discussion, the Böttcher coordinate may be extended until the domain reaches the free critical point $-a$. This maximal domain of definition, V, is the unbounded component of the complement of the equipotential passing through $-a$, which is a topological figure eight curve, crossing itself at $-a$, see Figure 12. Then the image $\phi(V)$ is the complement of D_r for some $r > 1$.

Definition 2.23. *Let p be a polynomial as above. For $t \in \mathbb{R}/\mathbb{Z}$, the **external ray***

25

of angle t *for p is defined as*

$$r_e(t) := \{\phi^{-1}(se^{2\pi it})|s > r\}.$$

We would like to have an appropriate concept of the landing of such rays on the Julia set J. For this, we must extend ϕ via analytic continuation inside of the equipotential through the free critical point. We are able to do this as long as we can choose disks on which to perform the continuation which do not contain any pre-images of the free critical point $-a$. If the landing point of such a ray of argument t exists, we will again denote it by $\lambda_e(t)$.
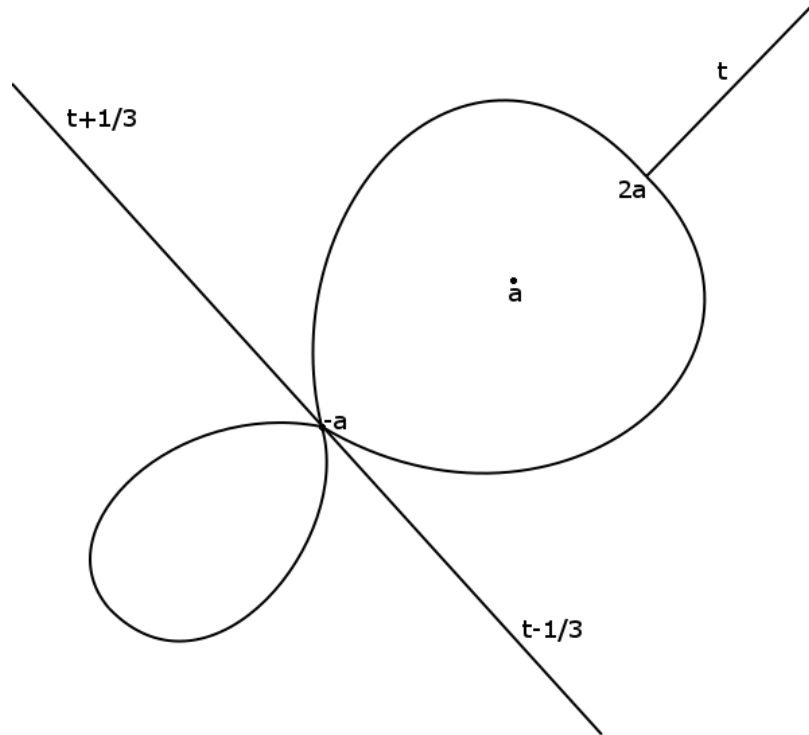
Figure 12. An illustration of a typical boundary of the maximal domain of definition of the Böttcher coordinate for a map on the external parameter ray of argument t, with important dynamical external rays marked.

Given a map F in any escape region of $\mathcal{S}_1$ or $\mathcal{S}_2$, the cocritical point $2a$ lies

on the equipotential passing through the free critical point $-a$. Therefore, there is a unique dynamic ray landing at $2a$. We use this unique dynamic ray to define parameter rays.

Definition 2.24. *The **external parameter ray of argument t**, denoted $R_e(t)$, consists of all maps F in the escape region for which the unique dynamic ray for F landing at the co-critical point $2a$ has argument t. If this parameter ray lands, we denote its landing map by $\Lambda_e(t)$.*

Recall that capital letters will be used for parameter rays, while lower case will be used in the case of dynamic rays. We make the important observation that for a map on the parameter ray of argument t, in the dynamic plane we have the external rays of arguments $t + \frac{1}{3}$ and $t - \frac{1}{3}$ crashing together at the free critical point $-a$, as shown in Figure 12.

We will make use of the following result of Roesch in [6, Theorem 6], which was originally proven by Faught in [8].

Theorem 2.25 (Roesch)**.** *The Boundary of the connectedness locus of $\mathcal{S}_1$ is locally connected at every point which is not in the boundary of a type D component.*

This then means that any external parameter ray which accumulates on a type A or C component indeed lands at a unique map on the boundary due to Theorem 2.15.

We will have a particular interest in certain external parameter rays. The following definition is adapted from [9].

Definition 2.26. *An argument $t \in \mathbb{R}/\mathbb{Z}$ is **co-periodic of co-period n** if either $t - \frac{1}{3}$ or $t + \frac{1}{3}$ is periodic of period n under tripling. A parameter ray whose argument is co-periodic of co-period n will be called co-periodic of co-period n.*

An argument $t \in \mathbb{R}/\mathbb{Z}$ is co-periodic of co-period n if and only if it can be written in the form

$$t = \frac{m}{3(3^n - 1)}$$

where m is relatively prime to 3, and n is minimal.

2.8   The Period q Decomposition of $\mathcal{S}_n$

For some $q \in \mathbb{N}$, let $Q \subset \mathbb{Q}/\mathbb{Z}$ be the set of all arguments periodic of period q under tripling. Such arguments have the form

$$\frac{m}{3^q - 1}$$

with q minimal. We now define the period q orbit portrait of a polynomial, similarly to Milnor in [10].

Definition 2.27. *Given a polynomial p, the period q orbit portrait is a partition of Q with each class consisting of all of the arguments landing at a common point.*

Now, given $n, q \in \mathbb{N}$, we will define the period q decomposition of $\mathcal{S}_n$

$$V(q) := \mathcal{S}_n \setminus \overline{\text{rays of co} - \text{period } q},$$

and will denote by $V_1, V_2, ..., V_m$ the connected components of $V(q)$, as in [7]. We will make use of the following result from [7, Theorem 3.1].

Theorem 2.28 (Bonifant and Milnor). *For each $p \in V_i$ and argument t which is periodic of period q under tripling in $\mathbb{R}/\mathbb{Z}$, the ray $r_e(t)$ for p lands at a repelling periodic point $z(p) \in J(p) \subset \mathbb{C}$. Furthermore, the map $p \mapsto z(p)$ from V_i to $\mathbb{C}$ is holomorphic. The orbit portrait for dynamic rays of period q is the same for all $p \in V_i$.*
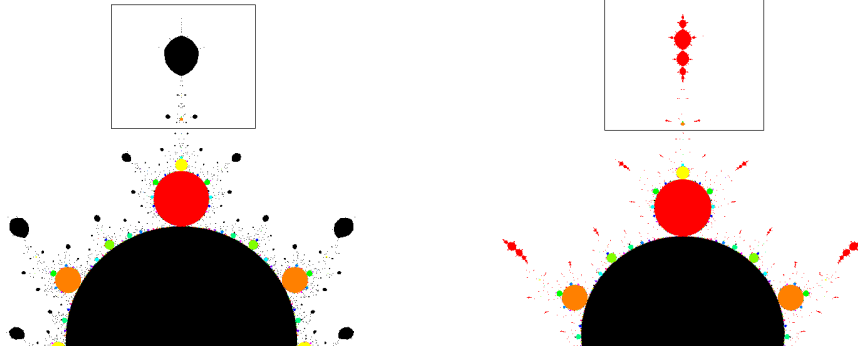
Figure 13. A region of $\mathcal{S}_1$ showing type C components homeomorphic to discs, and the corresponding image under $\widehat{\Psi}$ in $\mathcal{S}_2$, showing type C components homeomorphic to the basilica.
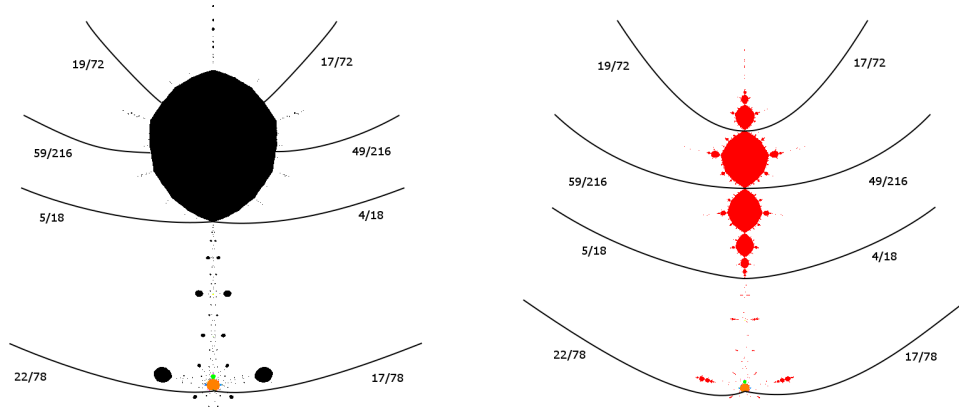
Figure 14. Magnifications of the areas indicated in Figure 13 with some external rays marked

2.9 A Conformal Isomorphism

For a general escape region $\mathcal{E}$ in any $\mathcal{S}_n$, there is a multiplicity $\mu_{\mathcal{E}} \in \mathbb{N}$, and a canonical isomorphism between $\mathcal{E}$ and the $\mu_{\mathcal{E}}$-fold cyclic covering of $\mathbb{C} \setminus \overline{\mathbb{D}}$, see [4, Lemma 5.9]. The escape regions in $\mathcal{S}_1$ and $\mathcal{S}_2$ all have multiplicity one, see [7], so that each is conformally isomorphic to the complement of the closed unit disc.

We will have particular interest in the conformal isomorphisms

$$\Phi_1 : \mathcal{E}_1 \to \mathbb{C} \setminus \overline{\mathbb{D}}, \text{ and}$$

$$\Phi_2 : \mathcal{E}_2^B \to \mathbb{C} \setminus \overline{\mathbb{D}},$$

29
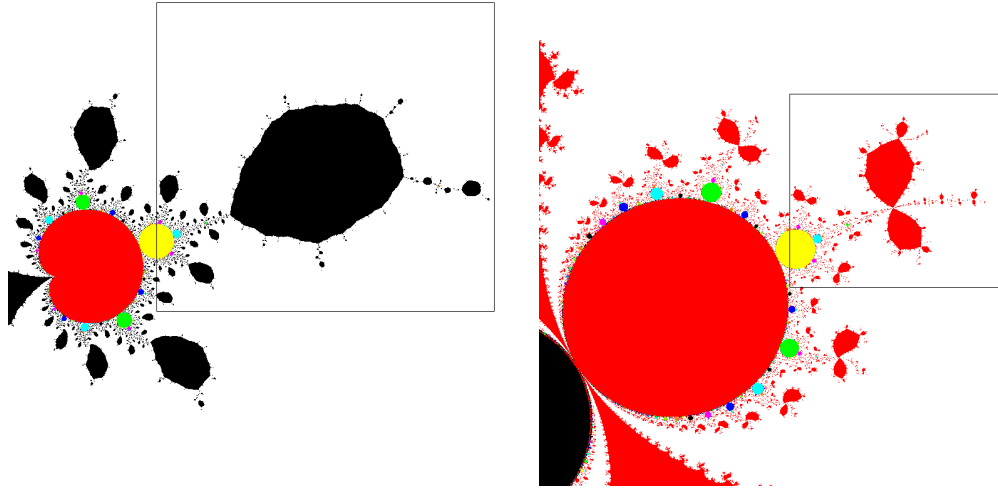
Figure 15. Another region of $\mathcal{S}_1$ and the corresponding image under $\widehat{\Psi}$ in $\mathcal{S}_2$.
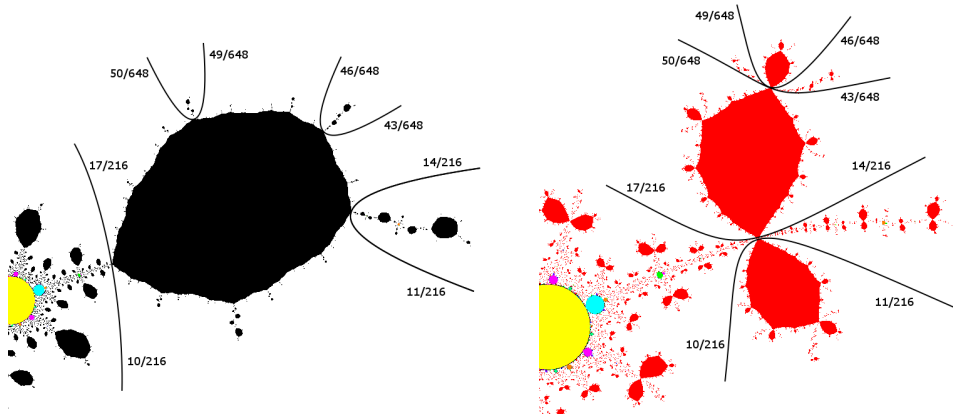
Figure 16. Magnifications of the areas indicated in Figure 15 with some external rays marked.

which are defined by mapping parameter rays to radial lines of corresponding argument. The composition

$$\Psi = \Phi_2^{-1} \circ \Phi_1 : \mathcal{E}_1 \to \mathcal{E}_2^B$$

is then a parameter ray preserving conformal isomorphism between the two escape regions. Let $\widetilde{\Psi}$ be the continuous extension of Ψ to the set of all maps on the boundary of a type A or C component of $\mathcal{C}(\mathcal{S}_1)$. Such an extension is well defined by Theorem 2.25. Now, we let $\widehat{\Psi}$ be the restriction of $\widetilde{\Psi}$, mapping the boundary of

components of types A and C in $\mathcal{S}_1$ to the boundary of corresponding components of types A, B, and C in $\mathcal{S}_2$. We are interested in the set of points on the boundary of type A or C components in $\mathcal{S}_1$ where $\widehat{\Psi}$ is injective. This will be explored in detail in Chapter 4. First, we must spend some time building tools and establishing facts about the basilica map.

List of References

[1] A. Douady and J. H. Hubbard, "The Orsay notes," Available at www.picard. ups-tlse.fr/~buff/OrsayNotes/OrsayNotes.pdf.

[2] J. Milnor, *Dynamics in One Complex Variable.* Princeton, New Jersey, United States of America: Princeton University Press, 2006.

[3] B. Branner and J. H. Hubbard, "The iteration of cubic polynomials Part I: The global topology of parameter space," *Acta Math.*, vol. 160, pp. 143–206, 1988.

[4] J. Milnor, "Cubic polynomial maps with periodic critical orbit, Part I," in *Complex Dynamics Families and Friends*, 2009, pp. 333–411.

[5] M. Rees, "Components of degree two hyperbolic rational maps," *Invent. Math.*, vol. 100, pp. 357–382, 1990.

[6] P. Roesch, "Hyperbolic components of polynomials with a fixed critical point of maximal order," *Ann. Sci. Ec. Norm. Sup.*, vol. 40, pp. 901–949, 2007.

[7] A. Bonifant, J. Kiwi, and J. Milnor, "Cubic polynomial maps with periodic critical orbit, Part II," *Conform. Geom. Dyn.*, vol. 14, pp. 68–112, 2010.

[8] D. Faught, "Local connectivity in a family of cubic polynomials," Ph.D. dissertation, Cornell University, 1992.

[9] A. Bonifant and J. Milnor, "Cubic polynomial maps with periodic critical orbit, Part III," 2010, manuscript.

[10] J. Milnor, "Periodic orbits, external rays, and the Mandelbrot set," in *Géometrie Complexe et Systémes Dynamiques*, 2000, pp. 277–333.

CHAPTER 3

The basilica map

We require some facts about the basilica map $z \mapsto z^2 - 1$. We will introduce the concepts of Hubbard trees and laminations for quadratic polynomials, with a particular focus on the basilica map. We will then discuss the basics of hybrid equivalence, and an important result of Branner and Hubbard.

3.1 Hubbard trees

The notion of a Hubbard tree was introduced by Douady and Hubbard in [1]. The following definitions are necessary to the concept of a Hubbard tree.

Definition 3.1. *Let p be a polynomial with critical points $z_0, z_1, ..., z_{n-1}$. The* **post-critical set** *is defined to be*

$$P(p) = \{p^i(z_j) \mid i \in \mathbb{N},\ j \in \mathbb{Z}_n\}.$$

The polynomial p is said to be **post-critically finite** *if $P(p)$ is a finite set.*

It follows that a polynomial is post-critically finite if and only if every critical point is pre-periodic.

Consider a post-critically finite polynomial p. We will follow Milnor and Poirier's appendix on Hubbard trees in [2], which is more general than we will need. Each Fatou component for p is conformally isomorphic to a disc, and is either periodic or pre-periodic due to Sullivan's non-wandering theorem, see [3]. Since we are considering a post-critically finite polynomial, it follows that each component contains a unique point which is either periodic or pre-periodic.

Definition 3.2. *Given a Fatou component of a post-critically finite polynomial, the unique periodic or pre-periodic point in that component will be referred to as the* **center** *of the component.*

In the standard disc model of hyperbolic geometry, a geodesic is an arc of a circle in the disc which meets the boundary of the disc at right angles, see Figure 17. Given a Fatou component F for a post-critically finite polynomial, we have a conformal isomorphism $\varphi : \mathbb{D} \to F$ mapping 0 to the center of F. Using this map, we may talk about hyperbolic geodesics in F, considering them as images under φ of the standard hyperbolic geodesics in $\mathbb{D}$.
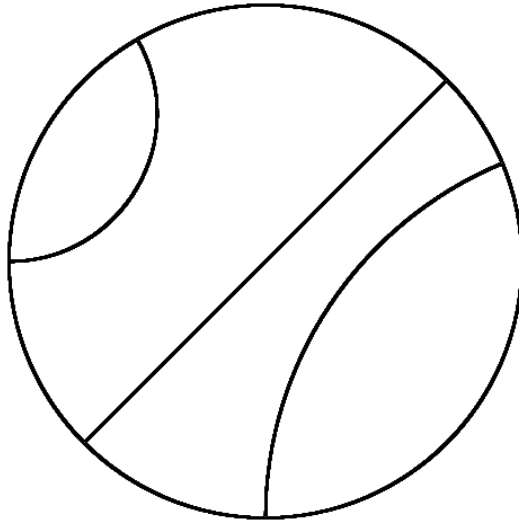
Figure 17. Hyperbolic geodesics in the standard disk model.

Definition 3.3. *Let p be a post-critically finite polynomial. A path in the filled Julia set $K(p)$ is **regulated** if its intersection with each Fatou component consists of at most two hyperbolic geodesics connecting the center of the component to a point on the boundary.*

Now, for a post-critically finite polynomial p, let S be the union of the set of critical points with the post-critical set $P(p)$. This is the smallest forward invariant set containing the critical points, and is finite by assumption. We now define the Hubbard tree.

Definition 3.4. *Let p be a post-critically finite polynomial. The **Hubbard tree** (sometimes called the minimal Hubbard tree) for p is the smallest set containing a regulated path between any two points of S, and will be denoted H_p.*
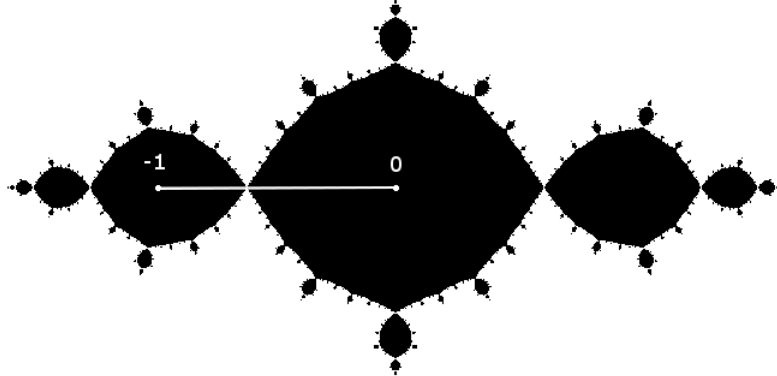
Figure 18. The basilica with its Hubbard tree highlighted.

The Hubbard tree is a topological tree (T, V), where V will be a specified set of vertices. Each critical and post-critical point for a post-critically finite polynomial is a vertex of its Hubbard tree, however the set of vertices is sometimes strictly larger. The valence $v(z)$ of a point in $z \in J(p)$, as defined in [4], will be the number of external rays for p landing at z. We then define $V := S \cup \{z \in T \cap J(p) | v(z) \geq 3\}$. For example, consider the unique value c_r in the first quadrant of $\mathbb{C}$ such that for $p_r(z) = z^2 - c_r$, we have $p_r^3(0) = 0$ (numerically, $c_r = .12256... + .74486...i$). The Julia set for this map is referred to as Douady's Rabbit, see Figure 19. The set S consists of the three points $0, c_r$, and $p_r(c_r)$, however V contains also the fixed point of valence 3 in $T \cap J(p_r)$ which is the landing point of the three external rays $r_e\left(\frac{1}{7}\right), r_e\left(\frac{2}{7}\right)$, and $r_e\left(\frac{4}{7}\right)$.

For a post-critically finite polynomial p with associated Hubbard tree (T, V),
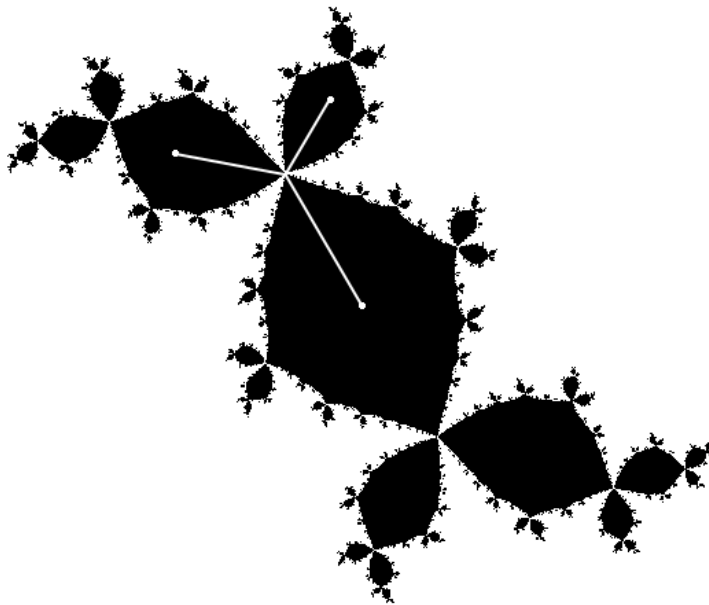
Figure 19. Douady's rabbit with its Hubbard tree highlighted. This tree requires four vertices, despite the map having three total critical and post-critical points.

the valence of points in $T \cap J(p)$ is very important. The following result of Tan Lei, [5, Proposition 4.3], expresses the reason for this, and will be useful in obtaining later results.

Theorem 3.5 (Tan Lei). *Every point z in the Julia set J of a monic post-critically finite polynomial p which is the landing point of more than one external ray eventually lands on the Hubbard tree of p under iteration of p.*

3.2 Laminations

Consider a polynomial p whose Julia set is connected and locally connected. We will define an associated equivalence relation on $\mathbb{R}/\mathbb{Z}$.

Definition 3.6. *The equivalence relation L which relates arguments $t, s \in \mathbb{R}/\mathbb{Z}$*

whenever $\lambda_e(t) = \lambda_e(s) \in J(p)$ *is called the* **lamination** *of* p.

The concept of a lamination is more general than what we will require, see [6]. A lamination can be visualized as a closed disc $\overline{D}$ with non-intersecting hyperbolic geodesics connecting the points on the boundary which are identified. Each arc in this model will be referred to as a leaf, and when necessary, we will use $\ell_{s,t}$ to denote the leaf connecting arguments s and t. The quotient $\overline{D}/L$ is homeomorphic to the filled Julia set $K(p)$ as explained in Dierk Schleicher's appendix to [6].

Definition 3.7. *Let a, b be the representatives in $[0, 1)$ of $t - s, s - t \in \mathbb{R}/\mathbb{Z}$. The* **length** *of the leaf connecting points at arguments t and s will be defined as* $\min\{a, b\}$.

Since, for a quadratic polynomial, forward iteration corresponds to doubling arguments of external rays, we expect that leaves should get longer under such iteration. There are important leaves for which this is not the case, which motivates the following definition, adapted from Thurston in [6, Definition II.6.2].

Definition 3.8. *A leaf ℓ of a lamination L for a quadratic polynomial is called* **principle** *if ℓ is at least as long as any of its forward images. For any lamination L, let M be the greatest length of any leaf of L. Any leaf of length M is a principal leaf. Unless $M = \frac{1}{2}$, L has two leaves of length M. The longest leaf or leaves we will call* **major** *leaves of L. The images of the major leaves of L coincide; this image will be called the* **minor** *leaf of L.*

Thurston comments that the minor leaf need not be a leaf at all. It could be a point, in which case we can get around this by considering a point to be a degenerate leaf. However, for the basilica map, the major leaves are $\ell_{\frac{1}{3},\frac{2}{3}}$ and $\ell_{\frac{1}{6},\frac{5}{6}}$, and the minor leaf therefore is exactly the major leaf $\ell_{\frac{1}{3},\frac{2}{3}}$.

We would like to describe an inductive process for finding the lamination of the basilica map. The process consists of finding all of the periodic rays which land together in the first step, and for each subsequent step, taking all preimages of all leaves from the previous step. Therefore, we need to describe how to find a preimage of a leaf. We have the following useful result, which also allows us to introduce some terminology.
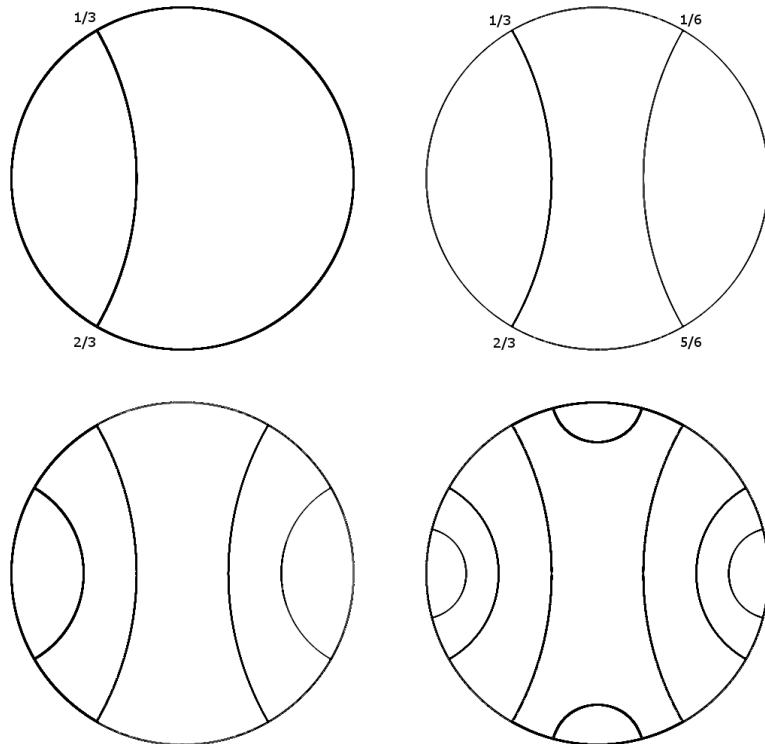
Figure 20. The first four steps of the inductive process for obtaining the lamination of the basilica.

Lemma 3.9. *Let L be the lamination of the basilica. Given an argument $t \in \mathbb{R}/\mathbb{Z}$ for which there is $n \in \mathbb{N}$ such that $2^n t \equiv \frac{1}{3}$, there is a unique $\widetilde{t} \in \mathbb{R}/\mathbb{Z}$, $\widetilde{t} \neq t$, such that L relates t and $\widetilde{t}$, i.e. $\lambda_e\left(\widetilde{t}\right) = \lambda_e(t)$.*

Proof. Let $p(z) = z^2 - 1$ be the basilica map, and $z_0 \in J(p)$ be the landing point of more than one external ray. From Theorem 3.5, we have that z_0 eventually lands

37

on the Hubbard tree H_p under iteration. The intersection $H_p \cap J(p)$ consists of a unique point, namely the common landing point of the external rays of arguments $\frac{1}{3}$ and $\frac{2}{3}$. Define $\alpha := \lambda_e\left(\frac{1}{3}\right) = \lambda_e\left(\frac{2}{3}\right)$, and let n be the minimal natural number such that $p^n(z_0) = \alpha$, and $\delta > 0$ be the distance between z_0 and the nearest center of a Fatou component. Choose ε with $0 < \varepsilon < \delta$. It then follows that $p^n|_{D(z_0,\varepsilon)}$ is a homeomorphism onto a neighborhood of α. Therefore, we may conclude that there is an argument t for which $\lambda_e(t) = z_0$ and $2^n t \equiv \frac{1}{3}$, as well as a unique corresponding $\widetilde{t}$ with $\lambda_e\left(\widetilde{t}\right) = z_0 = \lambda_e(t)$. $\qquad\square$
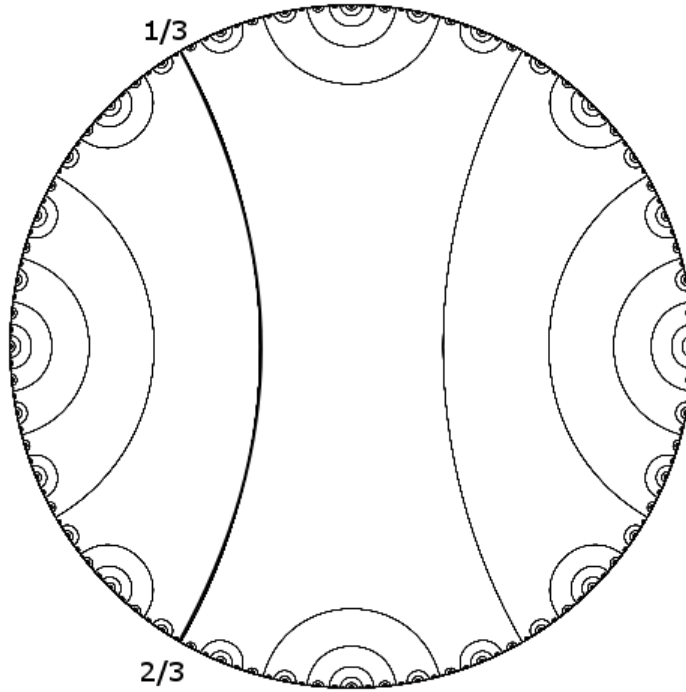
Figure 21. The lamination of the basilica.

Definition 3.10. *An argument $t \in \mathbb{R}/\mathbb{Z}$ will be called a basilica angle if there is $n \in \mathbb{N}$ such that $2^n t \equiv \frac{1}{3}$. If t is a basilica angle and $s \neq t$ is the unique argument in $\mathbb{R}/\mathbb{Z}$ such that s and t are related in the lamination of the basilica, then (s,t) will be referred to as a basilica pair.*

38

Considering Lemma 3.9, to find a preimage of a leaf $\ell_{s,t}$ of the lamination of the basilica, we first choose a preimage under doubling of one of the arguments, say t. We then identify this preimage with its unique partner, which is the preimage of s which is accessible from our preimage of t, in the sense that this new leaf created doesn't cross any existing leaves of the lamination. The lamination of the basilica is then obtained by starting with the major leaf $\ell_{\frac{1}{3},\frac{2}{3}}$ as the first step, then inductively taking all preimages of the leaves from the previous step.

Now, assume we are given a polynomial q with a fixed simple critical point z_0, whose immediate basin does not contain another critical point of q. Then for any component A of $\mathcal{A}_{z_0}$, the internal rays give us a natural way of viewing its boundary as $\mathbb{R}/\mathbb{Z}$ by associating each point with the argument of the internal ray landing there. This allows us to put the basilica lamination inside of the component by relating the landing points of internal rays $\lambda_i(t), \lambda_i(s) \in \partial A$ whenever (s, t) is a basilica pair. We may then consider the quotient of $\partial A = \mathbb{R}/\mathbb{Z}$ by this lamination as before, which turns the topological disc component A into a homeomorphic copy of the basilica. See Figure 22.
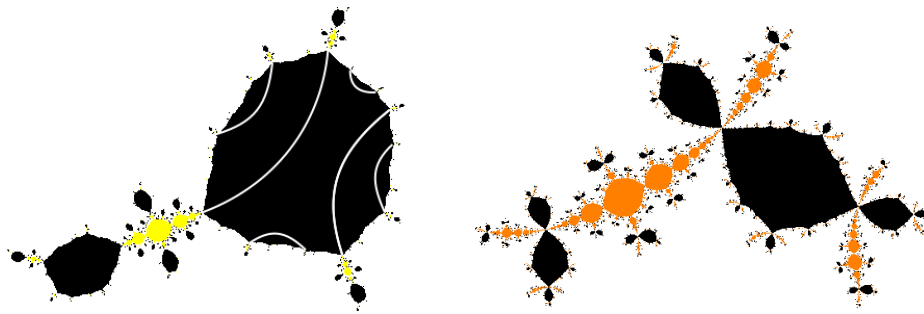
Figure 22. A map on the left with some identifications from the lamination of the basilica shown in a disc component of the filled Julia set, and the result on the right of the quotient by the basilica lamination.

3.3 Hybrid equivalence

We will require the concept of hybrid equivalence, introduced in [7], which will necessitate the ideas of both quasiconformal and polynomial-like mappings. We begin by considering an orientation preserving C^1 homeomorphism

$$w = f(z) = u(x + iy) + iv(x + iy)$$

from some region of $\mathbb{C}$ to another. We then have the standard partial derivatives $\frac{\partial f}{\partial x}$ and $\frac{\partial f}{\partial y}$, which we use to define the z and $\overline{z}$-derivatives

$$f_z = \frac{\partial f}{\partial z} := \frac{1}{2}\left(\frac{\partial f}{\partial x} - i\frac{\partial f}{\partial y}\right), \text{ and } f_{\overline{z}} = \frac{\partial f}{\partial \overline{z}} := \frac{1}{2}\left(\frac{\partial f}{\partial x} + i\frac{\partial f}{\partial y}\right).$$

Definition 3.11. *The quantity*

$$D_f(z) = \frac{|f_z| + |f_{\overline{z}}|}{|f_z| - |f_{\overline{z}}|} \geq 1$$

*is called the **dilatation** of f at the point z.*

Definition 3.12. *The map f is called **quasiconformal** if the dilatation function $D_f(z)$ is bounded over the domain of f.*

For more information, see [8].

Definition 3.13. *A **polynomial-like map** of degree d is a triple (f, U, V) where $U, V \subset \mathbb{C}$ are open and isomorphic to discs, with U relatively compact in V, and $f : U \to V$ is holomorphic and proper of degree d. We say that two polynomial-like maps (f, U_1, V_1) and (g, U_2, V_2) are **hybrid equivalent** if they are quasiconformally conjugate, and the conjugacy ϕ can be chosen to be conformal on $K(f) := \bigcap_{n \geq 0} f^{-n}(U)$*

We have the following specialization of an important result of Branner and Hubbard from [9, Theorem 5.3], although we will more closely follow Milnor's

restatement from [2, Theorem 5.15], which requires us first to define a kneading sequence.

Let p be a polynomial in any escape region of $\mathcal{S}_n$, lying on the parameter ray of argument t. Then the dynamical plane is separated into two components by the rays $r_e(t+\frac{1}{3})$ and $r_e(t-\frac{1}{3})$ together with the free critical point $-a$, and the point at infinity. We will label U_0 the component containing the marked critical point a, and the other we will label U_1. We then form a binary sequence $\sigma = (\sigma_1, \sigma_2, ...)$ from the orbit of the marked critical point a, by setting $\sigma_m = i$ whenever $p^m(a) \in U_i$. Since a is periodic of period n under p, this sequence is also periodic, having some period ℓ which divides n. This sequence σ will be referred to as the kneading sequence for the polynomial p. Recall that K_a refers to the component of the filled Julia set of p containing the marked critical point a.

Theorem 3.14 (Milnor). *For a polynomial p in an escape region of $\mathcal{S}_n$ for $n = 1, 2$, the restriction of p to a neighborhood of K_a is hybrid equivalent to a unique quadratic polynomial, which has periodic critical orbit of period $\frac{n}{\ell}$ where ℓ is the period of the kneading sequence for p.*

Remark. It is noted in [10] that [2, Theorem 5.15] is not true in its full generality. However, when considering small values of n (up to and including $n = 3$), the result holds as stated.

From [10], the kneading sequence is an invariant of each escape region, and furthermore each escape region of $\mathcal{S}_1$ and $\mathcal{S}_2$ is uniquely determined by its kneading sequence. Observing that a quasiconformal conjugacy necessarily preserves topology, this justifies our earlier terminology of referring to the escape regions in $\mathcal{S}_2$ as the disc region and the basilica region. For $F \in \mathcal{E}_2^B$, the topology of each nontrivial component of $K(F)$ is indeed that of the filled Julia set of the basilica map.

Lemma 3.15. *For a map $F = (r,t)_2^B \in \mathcal{E}_2^B$, there is a unique fixed point in J on the boundary of the Fatou components containing the marked critical point a, and its associated critical value v.*

Proof. From the Theorem of Milnor above, there is a neighborhood U of the main basilica component of $K(F)$ such that the restriction of F to U is hybrid equivalent to the basilica map $z \mapsto z^2 - 1$. This map has fixed points $z_0 = \frac{1}{2} + \frac{\sqrt{5}}{2}$ and $z_1 = \frac{1}{2} - \frac{\sqrt{5}}{2}$. The point z_1 is the only point on the boundary of the components containing the critical point 0 and its associated critical value -1. Therefore, in $J(F)$ there is a corresponding unique fixed point on the boundary of the Fatou components containing a and v. $\qquad\square$
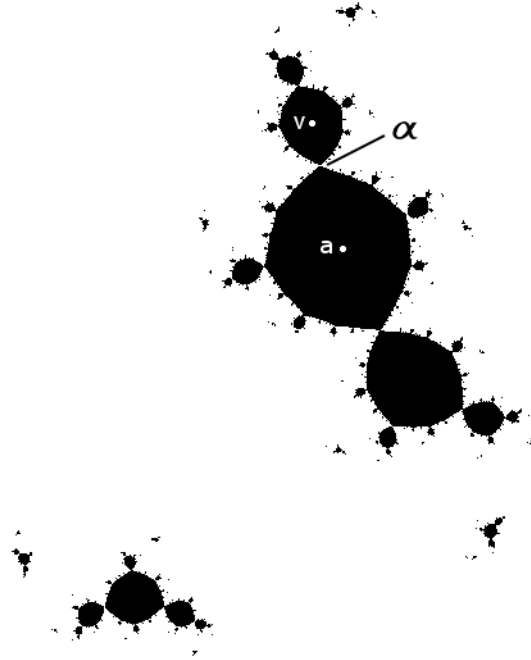
Figure 23. The filled Julia set of a map in $\mathcal{E}_2^B$ showing the placement of the fixed point α.

Definition 3.16. *For a polynomial $p \in \mathcal{E}_2^B$, we define α to be the fixed point described above.*

This fixed point α is of critical importance to the main results of this work, see Figure 23. Given a map $p \in \mathcal{E}_1$, it is at this point α in the filled Julia set of the image map under Ψ that we find two dynamical rays landing together which land at distinct points in the filled Julia set of p. We are then able to find all other dynamical identifications by taking preimages of this initial identification at α. By continuity, we extend this result to the boundary of $\mathcal{E}_1$ to obtain a similar result for $\widehat{\Psi}$. These dynamical identifications between maps on the boundaries of the connectedness loci then provide us with the information necessary to find the identifications in parameter space that we are looking for. The details are discussed in Chapter 4.

List of References

[1] A. Douady and J. H. Hubbard, "The Orsay notes," Available at www.picard. ups-tlse.fr/~buff/OrsayNotes/OrsayNotes.pdf.

[2] J. Milnor, "Cubic polynomial maps with periodic critical orbit, Part I," in *Complex Dynamics Families and Friends*, 2009, pp. 333–411.

[3] D. Sullivan, "Quasiconformal homeomorphisms and dynamics I: Solution of the Fatou-Julia problem on wandering domains," *Ann. Math.*, vol. 122, pp. 401–418, 1985.

[4] J. Milnor, "Periodic orbits, external rays, and the Mandelbrot set," in *Géometrie Complexe et Systémes Dynamiques*, 2000, pp. 277–333.

[5] L. Tan, "Branched coverings and cubic Newton maps," *Fund. Math.*, vol. 154, pp. 207–226, 1997.

[6] W. P. Thurston, "On the geometry and dynamics of iterated rational maps, with appendix by D. Schleicher," in *Complex Dynamics Families and Friends*, 2009, pp. 3–137.

[7] A. Douady and J. H. Hubbard, "On the dynamics of polynomial-like mappings," *Ann. Sci. Ec. Norm. Sup.*, vol. 18, pp. 287–343, 1985.

[8] L. Ahlfors, *Lectures on Quasiconformal Mappings.* Belmont, CA: Wadsworth, 1987.

[9] B. Branner and J. H. Hubbard, "The iteration of cubic polynomials Part II: Patterns and parapatterns," *Acta Math.*, vol. 169, pp. 229–325, 1992.

[10] A. Bonifant, J. Kiwi, and J. Milnor, "Cubic polynomial maps with periodic critical orbit, Part II," *Conform. Geom. Dyn.*, vol. 14, pp. 68–112, 2010.

CHAPTER 4

Identifications in Escape Regions

We begin with a way of representing maps in escape regions based on combinatorial data. We then obtain some results using this representation which will help us to describe the map $\widehat{\Psi}$. This will be helpful in obtaining our main results.

4.1 Preliminary Results

Lemma 4.1. *Let $\mathcal{E}$ be an escape region of multiplicity 1 in $\mathcal{S}_n$ for some $n \in \mathbb{N}$, and let $F \in \mathcal{E}$. Then F is uniquely determined by the ordered pair*

$$(\rho, t) \in \{x \in \mathbb{R} | x > 1\} \times \mathbb{R}/\mathbb{Z},$$

where $\rho = |\phi_F(2a_F)|$, and t is such that $r_e(t)$ lands at $2a_F$.

Proof. Since the multiplicity of the escape region $\mathcal{E}$ is 1, from a result of Milnor, [1, Lemma 5.9], we have that the covering map $\Phi : \mathcal{E} \to \mathbb{C} \setminus \overline{\mathbb{D}}$ defined by

$$\Phi(F) = \phi_F(2a_F)$$

is in fact a conformal isomorphism. For existence, let $F \in \mathcal{E}$. Then

$$\Phi(F) = \rho e^{2\pi i t} \in \mathbb{C} \setminus \overline{\mathbb{D}},$$

where $|\rho e^{2\pi i t}| = \rho = |\Phi(F)| = |\phi_F(2a_F)| > 1$ and $t \in \mathbb{R}/\mathbb{Z}$ with $\lambda_e(t) = 2a_F$, so

$$(\rho, t) \in \{x \in \mathbb{R} | x > 1\} \times \mathbb{R}/\mathbb{Z}$$

represents the map F.

Uniqueness follows from the fact that Φ is injective, so that $\Phi(F) = \Phi(F^*)$ implies $F = F^*$. $\qquad\square$

We will use $(\rho, t)_1$ and $(\rho, t)_2^B$ to denote the unique maps in $\mathcal{E}_1$ and $\mathcal{E}_2^B$, respectively, determined by (ρ, t). If the parameter ray of angle t lands, the landing map will be denoted $(1, t)$. The following gives a useful description of the map Ψ in terms of this combinatorial description of the maps.

Lemma 4.2. $\Psi((\rho, t)_1) = (\rho, t)_2^B$

Proof. We have the commutative diagram

$$\begin{array}{ccc} \mathcal{E}_1 & \xrightarrow{\Phi_1} & \mathbb{C} \setminus \overline{\mathbb{D}} \\ & \searrow^{\Psi} & \uparrow^{\Phi_2} \\ & & \mathcal{E}_2^B \end{array}$$

which defines $\Psi = \Phi_2^{-1} \circ \Phi_1$.

Let $\Psi((\rho, t)_1) = (\rho^*, t^*)_2^B$. By definition, both Φ_1 and Φ_2 map parameter rays to radial lines of corresponding argument. Therefore, we may conclude that Ψ preserves parameter rays, and that $t = t^*$. Further, by the definitions of ρ, ρ^*, and the maps Φ_1, Φ_2, and Ψ, we have

$$\rho = |\phi_F(2a_F)| = |\Phi_1(F)|, \text{ and}$$

$$\rho^* = |\phi_{\Psi(F)}(2a_{\Psi(F)})| = |\Phi_2(\Psi(F))| = |\Phi_1(F)| = \rho.$$

$\square$

At this point, we make a conjecture which will need to be assumed for the remainder of the work. This is an analogous result to Theorem 2.25 for the basilica escape region of $\mathcal{S}_2$.

Conjecture. *The boundary of $\mathcal{E}_2^B$ is locally connected at every point which is not in the boundary of a type D component.*

This then guarantees the existence of the landing map $(1, t)_2^B$ whenever the landing map $(1, t)_1$ exists. This is due to Theorem 2.15, which says that a conformal isomorphism extends to the boundary if and only if the boundary is locally

connected. Recall that $\widetilde{\Psi}$ is the continuous extension of the conformal isomorphism $\Psi : \mathcal{E}_1 \to \mathcal{E}_2^B$ to a subset of $\partial \mathcal{E}_1$, and that $\widehat{\Psi}$ is the restriction of $\widetilde{\Psi}$ to this subset.

Lemma 4.3. *If $t \in \mathbb{R}/\mathbb{Z}$ is such that $(1, t)_1$ is on the boundary of a type A or C component of $\mathcal{S}_1$, then $\widehat{\Psi}((1, t)_1) = (1, t)_2^B$*

Proof. From the local connectivity of type A and C components in $\mathcal{S}_1$ established in Theorem 2.25, as well as Theorem 2.15 of Carathéodory, we may conclude that each point on the boundary of such a component is the landing point of at least one parameter ray. Further, by Lemma 4.2, and the fact that $\widetilde{\Psi}$ is the continuous extension of Ψ to the boundary of $\mathcal{E}_1$ and $\widehat{\Psi}$ is the restriction of $\widetilde{\Psi}$ to that boundary, we have

$$\widehat{\Psi}((1, t)_1) = \widetilde{\Psi}((1, t)_1) = \widetilde{\Psi}\left(\lim_{\rho \to 1}(\rho, t)_1\right) = \lim_{\rho \to 1}\widetilde{\Psi}((\rho, t)_1)$$

$$= \lim_{\rho \to 1}\Psi((\rho, t)_1) = \lim_{\rho \to 1}(\rho, t)_2^B = (1, t)_2^B,$$

thus the result is established. $\qquad\qquad\square$

4.2 Behavior of the Conformal Isomorphism

We would like to now describe the identifications that are made by Ψ in sending a map $(\rho, t)_1$ to its image $(\rho, t)_2^B$.

Recall the unique fixed point α on the boundaries of the Fatou components containing a and its associated critical value v from Definition 3.16. Since the components containing a and v form a two-cycle, the arguments of the rays landing at α must be periodic under tripling with period two. The possible arguments of pairs of rays landing at α are then $\left\{\frac{1}{8}, \frac{3}{8}\right\}$, $\left\{\frac{2}{8}, \frac{6}{8}\right\}$, and $\left\{\frac{5}{8}, \frac{7}{8}\right\}$. We will narrow down as much as possible for each map in $\mathcal{E}_2^B$ which pairs of period two rays could possibly land at α.

Lemma 4.4. *Given any map F on the parameter ray $R_e(t)$ in either $\mathcal{E}_1$ or $\mathcal{E}_2^B$, if the dynamic external ray $r_e(s)$ lands on the main component of $K(F)$, then $s \in (t - \frac{1}{3}, t + \frac{1}{3})$.*

Proof. As we saw in defining a kneading sequence, the rays $r_e(t - \frac{1}{3})$ and $r_e(t + \frac{1}{3})$, together with the free critical point $-a$ and the point at ∞, cut the Riemann sphere into two components. We will again label these components U_0 and U_1 as before, where U_0 is the component containing the marked critical point a, see Figure 24. Any ray with argument other than $t - \frac{1}{3}, t + \frac{1}{3}$ lies entirely in one of these components, since the crossing of rays would violate the injectivity of the Böttcher coordinate. The main component of $K(F)$ contains a, and therefore lies entirely in U_0, hence any ray landing on this main component must lie entirely in U_0 as well. The rays satisfying this property are precisely those of argument $s \in (t - \frac{1}{3}, t + \frac{1}{3})$. $\square$

Corollary 4.5. *Any pair of rays landing at α for a map $(\rho, t)_2^B$ must have both arguments in $(t - \frac{1}{3}, t + \frac{1}{3})$.*

Proof. Since α is on the main basilica component K_a of $K((\rho, t)_2^B)$, as shown in Figure 24, this follows directly from Lemma 4.4. $\square$

Lemma 4.6. *At most two pairs of period two rays could possibly land at α for any given $(\rho, t)_2^B \in \mathcal{E}_2^B$.*

Proof. Any arc containing all six period two arguments will necessarily have length greater than $\frac{2}{3}$. Therefore, by Corollary 4.5, at least one pair must always be excluded. $\square$

We will now decompose $\mathcal{E}_2^B$ into regions depending on how many pairs of rays can possibly land at α. In regions where only one pair of rays is possible, it follows
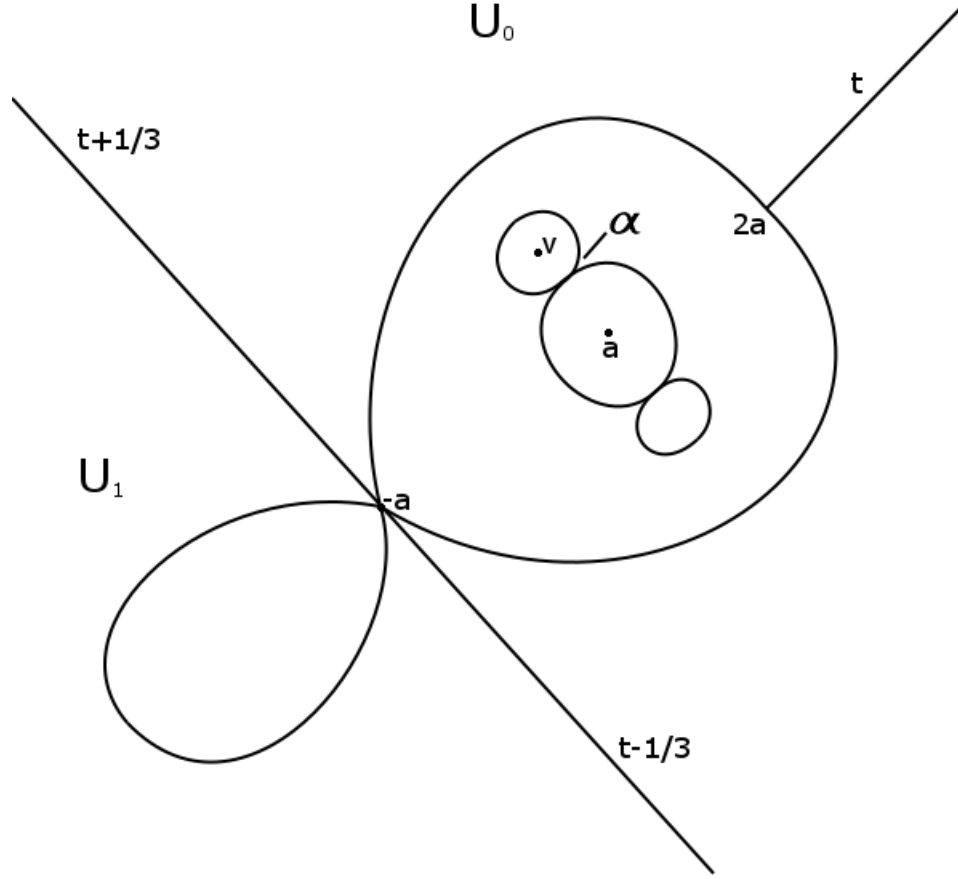
Figure 24. An updated version of Figure 12 for a map in $\mathcal{E}_2^B$. The same applies to a map in $\mathcal{E}_1$ with a disc in place of the main basilica component illustrated.

that those rays must land at α. We will further show that in regions where two pairs are possible, all four of the rays from these two possible pairs do indeed land at α.

Definition 4.7. *We will define the set* $W := \bigcup_{i=1,2,3,4} W_i$, *where* W_1 *will consist of all maps in* $\mathcal{E}_2^B$ *on parameter rays of argument* $t \in (\frac{1}{24}, \frac{2}{24})$, *and* W_2, W_3, *and* W_4 *are defined similarly with the intervals* $(\frac{10}{24}, \frac{11}{24}), (\frac{13}{24}, \frac{14}{24})$, *and* $(\frac{22}{24}, \frac{23}{24})$, *respectively, see Figure 25.*

We will require the following result which explains what happens on the boundary ∂W. Note that this boundary consists of eight parameter rays, all of
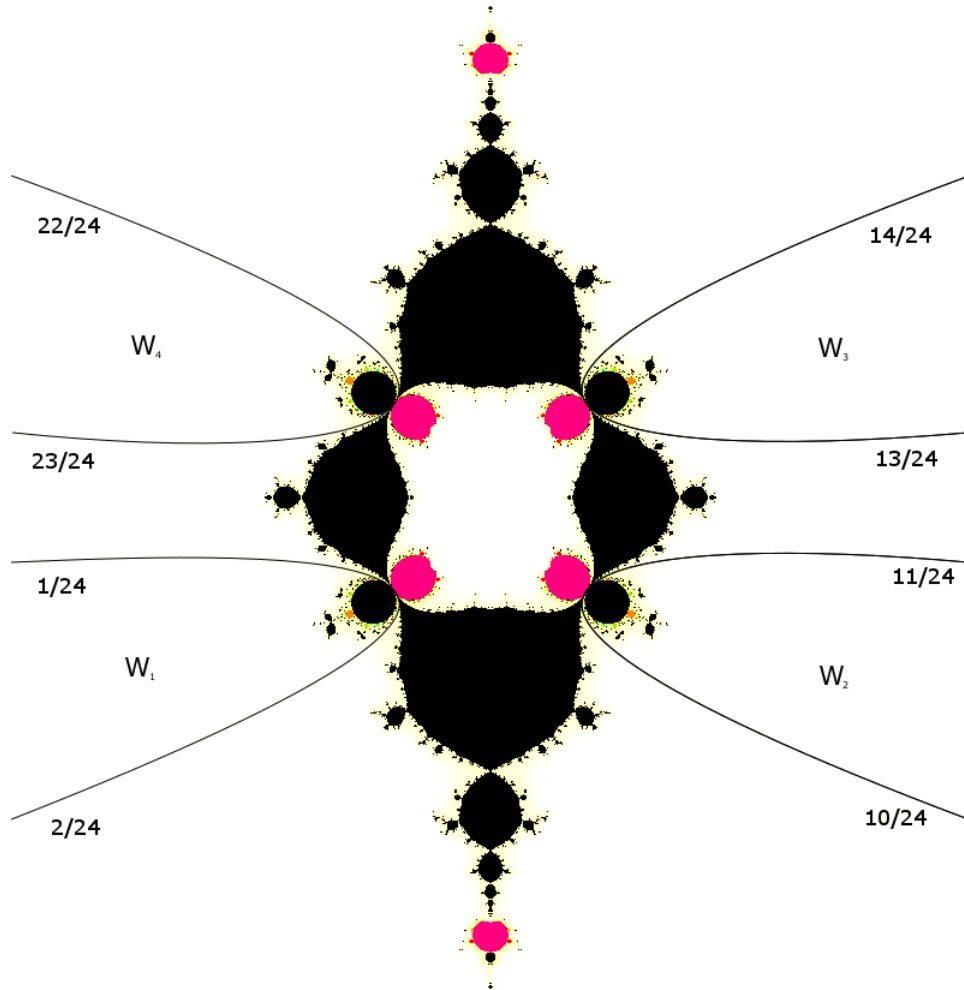
Figure 25. $\mathcal{S}_2$ with the basilica escape region decomposed into regions according to the number of rays landing at the fixed point α.

which are co-periodic of co-period two.

Lemma 4.8. *Suppose $F \in R_e(t) \subset \mathcal{E}_2^B$. Then all period two dynamic rays land on $J(F)$ if and only if $t \in \mathbb{R}/\mathbb{Z}$ is not co-periodic of co-period two.*

Proof. Let $F \in R_e(t)$. Suppose first that t is co-periodic of co-period two. Then one of the dynamic rays $r_e(t+\frac{1}{3})$ and $r_e(t-\frac{1}{3})$ is a period two ray which crashes into the free critical point $-a$ and therefore does not land on $J(F)$. Conversely, suppose

50

that there is a period two dynamic ray $r_e(\tilde{t})$ which does not land. Then there is a minimal $n \in \mathbb{N}$ such that $F^{-n}(-a) \in r_e(\tilde{t})$. Taking forward iterates, it then follows that one of the rays $r_e(\tilde{t})$ or $r_e(3\tilde{t})$, depending on the parity of n, crashes into the free critical point $-a$. This implies that $\tilde{t} \in \{t - \frac{1}{3}, t + \frac{1}{3}\}$ or $3\tilde{t} \in \{t - \frac{1}{3}, t + \frac{1}{3}\}$, and therefore that t is co-periodic of co-period two by definition. $\qquad\square$

We finish off the decomposition of the escape region $\mathcal{E}_2^B$ into regions depending on the number of possible rays landing at α with the following result.

Lemma 4.9. *For $(\rho, t)_2^B \in \mathcal{E}_2^B \setminus W$, there is exactly one possible pair of period two rays landing at α, and for $(\rho, t)_2^B \in W$, there are exactly two possible pairs of period two rays which land at α.*

Proof. First assume that $t \in (\frac{23}{24}, \frac{13}{24})$, refer to figure 25 to visualize which maps we are considering. For such angles we find that $t + \frac{1}{3} \in (\frac{7}{24}, \frac{7}{8})$ and $t - \frac{1}{3} \in (\frac{5}{8}, \frac{5}{24})$. Therefore, at least one of the angles from the pair $\{\frac{5}{8}, \frac{7}{8}\}$ is in the interval $(t + \frac{1}{3}, t - \frac{1}{3})$, which excludes this pair from landing at α by Corollary 4.5. Similarly, we may exclude the pair $\{\frac{1}{8}, \frac{3}{8}\}$ exactly when $t \in (\frac{11}{24}, \frac{1}{24})$, and the pair $\{\frac{2}{8}, \frac{6}{8}\}$ exactly when $t \in (\frac{2}{24}, \frac{10}{24})$ or $t \in (\frac{14}{24}, \frac{22}{24})$. On the co-period 2 rays which bound W, we know from Lemma 4.8 that one of the two possible pairs remaining is excluded by means of one of the rays in the pair crashing into $-a$. Considering all of these exclusions at once, the result is proven, and we have Figure 26 showing which pairs land at α in each region of $\mathcal{E}_2^B$. $\qquad\square$

We use the previous result to get an analogous result for the unique escape region $\mathcal{E}_1$ in $\mathcal{S}_1$, which will be important to our main results. Recall that for a map $F \in \mathcal{S}_n$, $\widehat{\mathcal{A}}_a$ is the immediate basin of attraction of the marked critical point a, that is, the connected component containing a of the set of all points whose orbits converge to a under iteration of F.
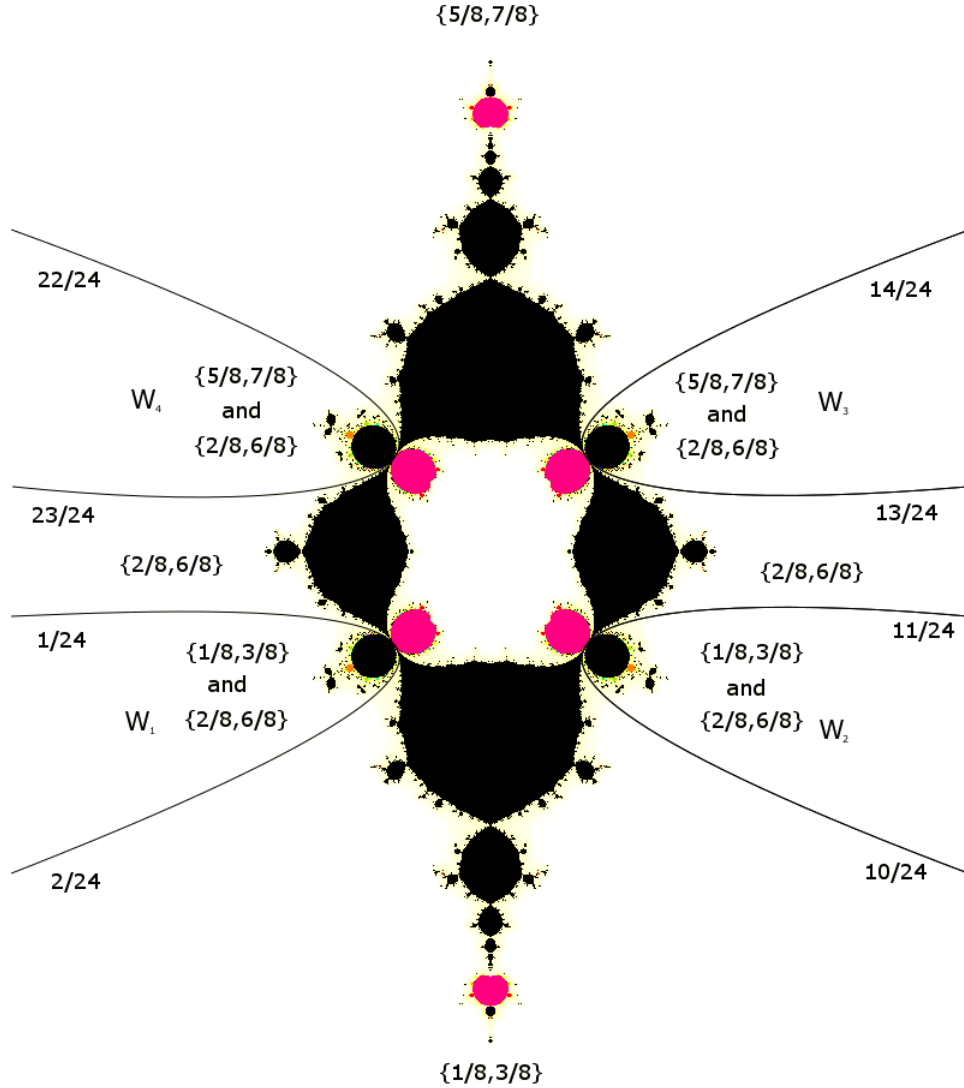
Figure 26. The pairs of rays landing at α in each piece of the basilica escape region.

Lemma 4.10. *For $(\rho, t)_1 = \Psi^{-1}((\rho, t)_2^B)$, if $(\rho, t)_2^B \in \mathcal{E}_2^B \setminus W$, then there is exactly one possible pair of period two rays landing on $\partial \widehat{\mathcal{A}}_a$, and if $(\rho, t)_2^B \in W$, then there are exactly two possible pairs of period two rays which land on $\partial \widehat{\mathcal{A}}_a$.*

Proof. By Lemma 4.4, any pair of period two rays landing on $\partial \widehat{\mathcal{A}}_a$ must have both arguments in $(t - \frac{1}{3}, t + \frac{1}{3})$. The rest of the argument then follows similarly to that of Lemma 4.9. $\square$
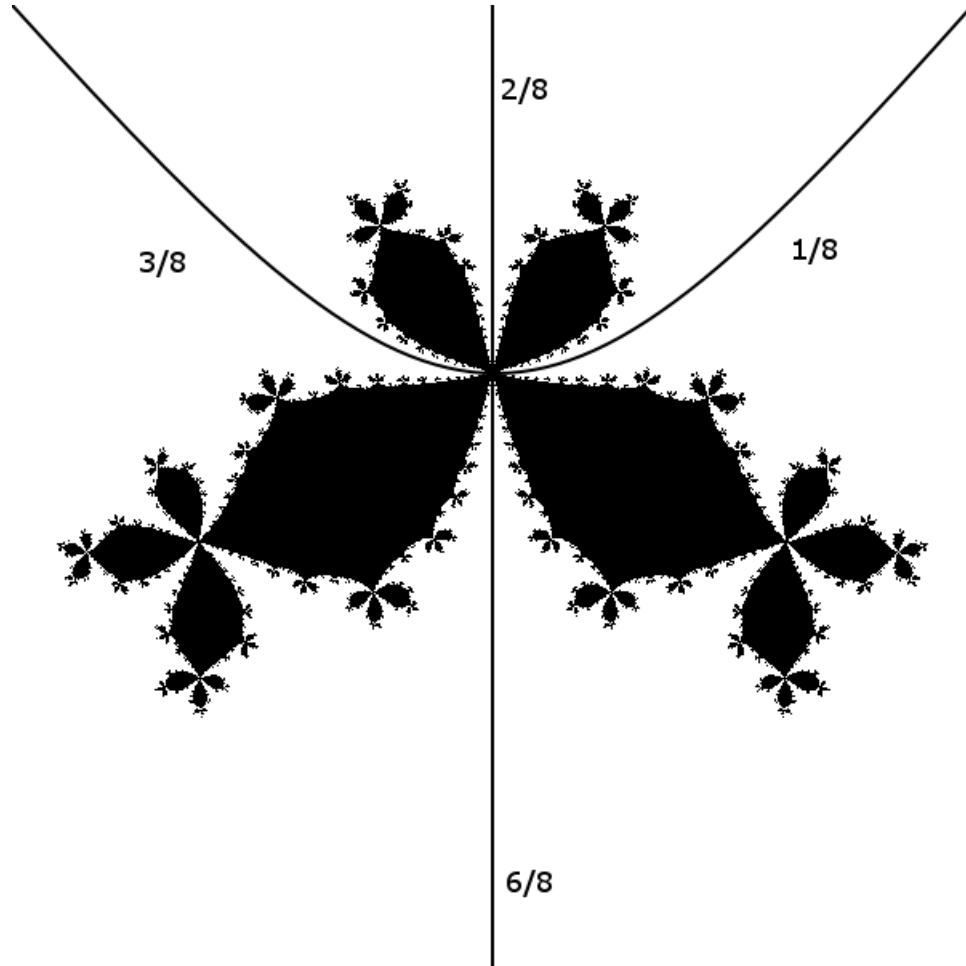
Figure 27. The Julia set of the map at the center of the period two hyperbolic component contained in the same component of the period two decomposition of $\mathcal{S}_2$ as the set W_1, with period two external rays which land together marked.

Now that we have our decomposition of the escape region $\mathcal{E}_2^B$ which tells us what pairs of period two rays could possibly land at the fixed point α, we would like to say something about which possible pairs actually do land at this point. When only one pair is possible, both rays in the pair must land at α, and the following result says that when there are two possible pairs, all four possible rays do indeed land at α as well.

Lemma 4.11. *For $(\rho, t)_2^B \in W$, let $\{t_1, t_2\}$ and $\{t_3, t_4\}$ be the two pairs of argu-*

ments of the rays not excluded from landing at α. Then we have

$$\lambda_e(t_i) = \alpha \ \text{ for } \ i = 1, 2, 3, 4.$$

Proof. Choose any $(\rho, t)_2^B \in W_1$. For this map we have $t_1 = \frac{1}{8}$, $t_2 = \frac{3}{8}$, $t_3 = \frac{2}{8}$, and $t_4 = \frac{6}{8}$. From Theorem 2.28 of Bonifant and Milnor, we know that $(\rho, t)_2^B$ has the same orbit portrait as any other map in the same component V_i of the period 2 decomposition of $\mathcal{S}_2$. Consider the unique post-critically finite polynomial p in the period two hyperbolic component in V_i, see Figure 27. For this map, the rays of arguments t_1, t_2, t_3, and t_4 all land together at a common fixed point on the boundaries of the Fatou components containing the marked critical point a_p and its associated critical value v_p. Therefore, we conclude that for $(\rho, t)_2^B$,

$$\lambda_e(t_i) = \alpha \ \text{ for } \ i = 1, 2, 3, 4.$$

$\square$

The following result establishes one of the most essential pieces of this work, namely that any pair of period two dynamic rays which land at the fixed point α in the Julia set of a map $\Psi(F) \in \mathcal{E}_2^B$ corresponds with a pair of dynamic rays for the map $F \in \mathcal{E}_1$ which land at distinct points in a two cycle on the boundary of the main disc component of the filled Julia set of F.

Lemma 4.12. *Given $F = (\rho, t)_1 \in \mathcal{E}_1$ and $s, \tilde{s} \in \mathbb{R}/\mathbb{Z}$ a two cycle under tripling for which $\lambda_e^{\Psi(F)}(s) = \lambda_e^{\Psi(F)}(\tilde{s}) = \alpha$ in $K(\Psi(F))$, we have $\lambda_e^F(s) \neq \lambda_e^F(\tilde{s})$ form a two cycle on $\partial \widehat{\mathcal{A}}_a \in K(F)$.*

Proof. There are two cases. First, suppose $\Psi(F) \in \mathcal{E}_2^B \setminus W$. Then by Lemma 4.10, we have exactly one pair of period two rays which could possibly land on $\partial \widehat{\mathcal{A}}_a$.
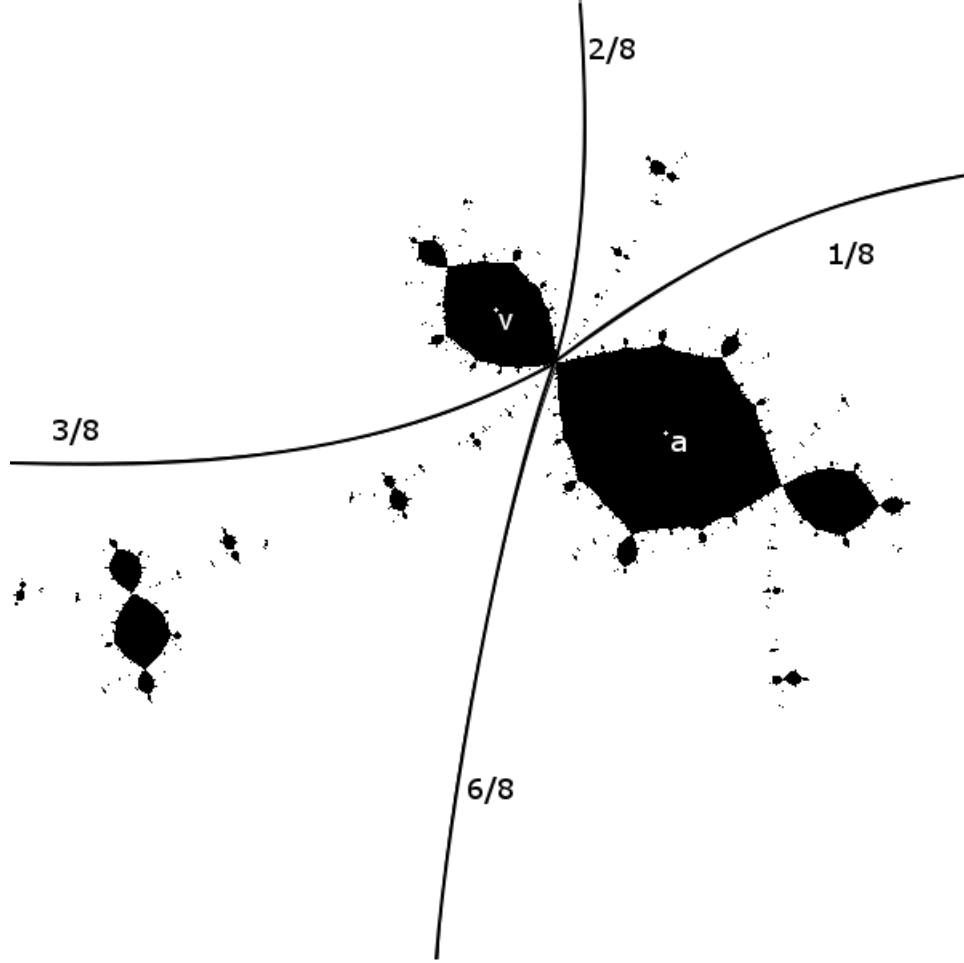
Figure 28. A Julia set from W_1 showing the four rays landing at the fixed point α.

Since Figure 12 applies to both $(\rho, t)_1$ and $(\rho, t)_2^B$, it follows that if $s, \tilde{s}$ are such that $\lambda_e^{\Psi(F)}(s) = \lambda_e^{\Psi(F)}(\tilde{s}) = \alpha$ in $K(\Psi(F))$, then the pair $\{s, \tilde{s}\}$ is the only pair of period two rays for which it is possible that $\lambda_e^F(s), \lambda_e^F(\tilde{s}) \in \partial \widehat{\mathcal{A}}_a$. Since we have the two cycle $\lambda_i^F(\frac{1}{3}), \lambda_i^F(\frac{2}{3}) \in \partial \widehat{\mathcal{A}}_a \subset J(F)$, it follows that these points must be the landing points of a pair of period two external rays, and therefore we must have the set equality

$$\left\{\lambda_e^F(s), \lambda_e^F(\tilde{s})\right\} = \left\{\lambda_i^F\left(\frac{1}{3}\right), \lambda_i^F\left(\frac{2}{3}\right)\right\} \subset \partial \widehat{\mathcal{A}}_a.$$

For the second case, suppose $\Psi(F) \in W$, and first assume that $\Psi(F) \in W_1$. The remaining cases then follow similarly. In this case, for the two pairs, $\left\{\frac{1}{8}, \frac{3}{8}\right\}$

and $\left\{\frac{2}{8}, \frac{6}{8}\right\}$ of period two rays, we have

$$\lambda_e^{\Psi(F)}\left(\frac{1}{8}\right) = \lambda_e^{\Psi(F)}\left(\frac{3}{8}\right) = \lambda_e^{\Psi(F)}\left(\frac{2}{8}\right) = \lambda_e^{\Psi(F)}\left(\frac{6}{8}\right) = \alpha.$$

By Theorem 2.28, the period two orbit portrait of F is the same as that of any other map in the same component of the period two decomposition of S_1. In this component we have the $\frac{1}{8}$ and $\frac{2}{8}$ rays landing at a common point, as well as the $\frac{3}{8}$ and $\frac{6}{8}$ rays, see Figure 29. Therefore, we have the two cycle

$$\lambda_e^F\left(\frac{1}{8}\right) = \lambda_e^F\left(\frac{2}{8}\right) \longleftrightarrow \lambda_e^F\left(\frac{3}{8}\right) = \lambda_e^F\left(\frac{6}{8}\right) \in \partial\widehat{\mathcal{A}}_a.$$

The proof follows similarly assuming $\Psi(F)$ is in any other W_i. $\qquad\square$

We are now prepared to obtain a very important result. The purpose of this result is to take a step towards describing the behavior of $\widehat{\Psi}$, by first describing this desired behavior for Ψ. This behavior of Ψ can be pictured as taking each of the disc components of the filled Julia set $K(F)$ for a map $F \in \mathcal{E}_1$, and replacing them with homeomorphic copies of the basilica in order to obtain a topological object which is homeomorphic to $K(\Psi(F))$. The intention of the main results is then to extend this result on the behavior of Ψ to the boundary in order to describe the behavior of $\widehat{\Psi}$. In order to do this, we will have to split up into separate cases based on whether we are on the boundary of a type A or C component of $\mathcal{S}_1$. The remainder of our main results will apply the dynamical information obtained on the boundary in order to describe what is happening topologically in parameter space. Here we are following the words of Adrien Douady, who said

> "we sow the seeds in the dynamical plane, and reap the harvest in the parameter plane."

Lemma 4.13. *Given $F = (\rho, t)_1 \in \mathcal{E}_1$, $K(\Psi(F))$ is homeomorphic to the quotient of $K(F)$ obtained by making the identifications from the lamination of the basilica along the internal rays of each disc component of $K(F)$.*
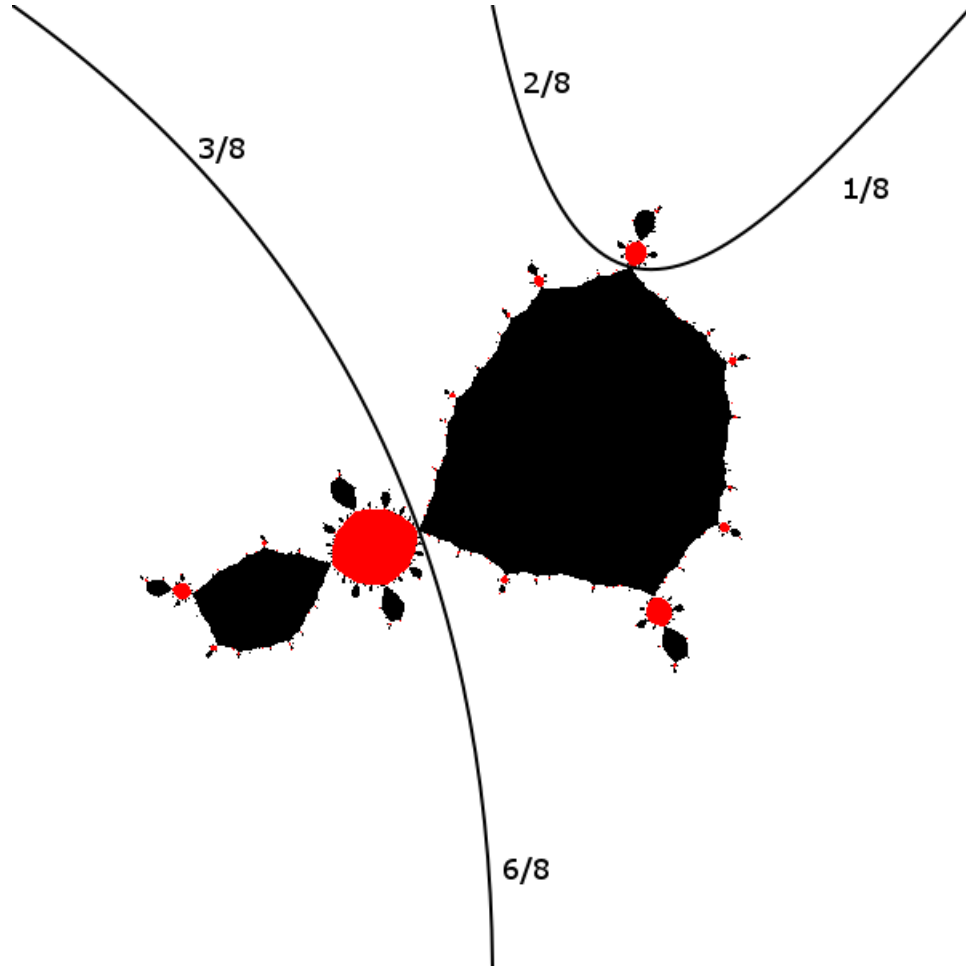
Figure 29. The Julia set of a map from the component of the period two decomposition of $\mathcal{S}_1$ which contains the entire preimage under Ψ of $W_1 \subset \mathcal{S}_2$.

Proof. Consider a pair of rays in the same orbit landing together at the point $\alpha \in K(\Psi(F))$. The corresponding dynamic rays in F of the same arguments must land at a two cycle on the boundary of the main disc component of $K(F)$ by Lemma 4.12. These landing points must then be the landing points of the $\frac{1}{3}$ and $\frac{2}{3}$ internal rays of this component, as these are the only period two internal rays. Let $r_e(t), r_e(\tilde{t})$ denote this pair of external rays of $K(F)$. Since these rays land together at α in $K(\Psi(F))$, this is an identification corresponding with the leaf $\ell_{\frac{1}{3},\frac{2}{3}}$ of the lamination of the basilica along the internal rays of the immediate basin of a. Without loss of generality, assume $\lambda_e(t) = \lambda_i(\frac{1}{3})$ and $\lambda_e(\tilde{t}) = \lambda_i(\frac{2}{3})$.

The three preimages of $r_e(t)$ must land at preimages of $\lambda_i(\frac{1}{3})$. These preimages are $\lambda_i(\frac{2}{3})$, $\lambda_i(\frac{1}{6})$, and a point off of the main component which we will disregard for now. Each of these landing points of internal rays is also the landing point of a corresponding external ray. We have $\lambda_e(\tilde{t}) = \lambda_i(\frac{2}{3})$, and we denote by t_1 the argument for which $\lambda_e(t_1) = \lambda_i(\frac{1}{6})$. We similarly find an argument $\tilde{t}_1$ such that $\lambda_e(\tilde{t}_1) = \lambda_i(\frac{5}{6})$, which is a preimage of the point $\lambda_i(\frac{2}{3})$. Now, in $K(\Psi(F))$, we know that there is exactly one preimage of α under $\Psi(F)$ in the main basilica component other than α itself, and it follows that this point is $\lambda_e(t_1) = \lambda_e(\tilde{t}_1)$. This identification of external rays corresponds to the leaf $\ell_{\frac{1}{6}, \frac{5}{6}}$ of the lamination of the basilica along the internal rays of the immediate basin of a. We find further identifications by taking preimages. We choose an internal argument where the previous identification occurred, say $\frac{1}{6}$, and further choose one of its preimages, say $\frac{1}{12}$. At this preimage, there is a corresponding external argument t_2 with $\lambda_i(\frac{1}{12}) = \lambda_e(t_2)$ in $K(F)$, for which, similarly to above, we can find another external argument $\tilde{t}_2$ for which $\lambda_e(t_2) = \lambda_e(\tilde{t}_2)$ in $K(\Psi(F))$, with $\tilde{t}_2$ landing at the same point as an appropriate preimage of $\lambda_i\left(\frac{5}{6}\right)$ in $K(F)$. By Lemma 3.9 there is exactly one possible internal argument to pair up with, in this case $\frac{11}{12}$. Continuing to find all preimages, this corresponds exactly with the inductive process for putting the lamination of the basilica in this component of $K(F)$. Now, we consider the preimage of $\lambda_i(\frac{1}{3}) \in J(F)$ off the main component, which was disregarded earlier. We similarly find an identification of external rays which produces the leaf $\ell_{\frac{1}{3}, \frac{2}{3}}$ of the basilica lamination in this preimage component. By pulling back all identifications to all preimage components of the filled Julia set, we find all of the identifications we have asserted. It then follows from Theorem 3.14 that there are no further identifications. $\qquad\square$

4.3 Main results

We begin with our main results by extending the result of Lemma 4.13 to the boundary to obtain a similar result describing how to obtain $K(\widehat{\Psi}(F))$ topologically from $K(F)$.

We have the following important corollary to Theorem 2.28. It essentially says that the fixed point α for maps in $\mathcal{E}_2^B$ persists in the landing map of any ray which is not co-periodic of co-period two. This is helpful for extending our results on identifications to the boundary of the escape region $\mathcal{E}_2^B$. The co-period two case will be handled separately later.

Lemma 4.14. *Suppose $t \in \mathbb{R}/\mathbb{Z}$ is not co-periodic of co-period two. The map $(1,t)_2^B \in \partial\mathcal{E}_2^B$ has a unique fixed point in J on the boundary of the Fatou components containing the marked critical point a, and its associated critical value v. Furthermore, the rays which land at this fixed point are exactly those which land at the fixed point α for any map $(\rho,t)_2^B \in \Lambda_e(t) \subset \mathcal{E}_2^B$.*

Proof. Suppose t is not co-periodic of co-period two. The landing point $(1,t)_2^B$ is in the same component of the period two decomposition as the rest of the ray $R_e(t)$. Therefore, by Theorem 2.28, the dynamic rays which land together at α for any map along the parameter ray $R_e(t)$ still land together at a fixed point in the landing map $(1,t)_2^B$. $\qquad\square$

We will continue to refer to this unique fixed point as α for maps on the boundary just as we did for maps in the escape region.

The following result accomplishes our goal of extending the behavior result for Ψ obtained in Lemma 4.13 to the map $\widehat{\Psi}$ which maps between boundaries of escape regions. The first part deals with landing points of parameter rays which are not co-periodic. For such maps, the free critical point $-a$ is in the Julia set, and every component of the filled Julia set is a component of the basin of attraction

of the marked critical point a. The second part then deals with landing points of co-periodic parameter rays, which are parabolic maps. For these maps, $-a$ belongs to a parabolic basin, and the filled Julia set consists of the basin of attraction of a as well as the parabolic basins.

Theorem 4.15. *Given $F = (1,t)_1 \in \partial \mathcal{E}_1$.*

1. If $R_e(t)$ is not co-periodic, $K(\widehat{\Psi}(F)) = K((1,t)_2^B)$ is homeomorphic to the quotient of $K(F)$ obtained by making the identifications from the lamination of the basilica along the internal rays of every Fatou component of $K(F)$.

2. If $R_e(t)$ is co-periodic, $K(\widehat{\Psi}(F)) = K((1,t)_2^B)$ is homeomorphic to the quotient of $K(F)$ obtained by making the identifications from the lamination of the basilica along the internal rays of the Fatou components of $K(F)$ which make up the basin of attraction $\mathcal{A}_{a_F}$ of the marked critical point a_F for F.

Proof. Let $F = (1,t)_1 \in \partial \mathcal{E}_1$.

1. Assume that $R_e(t)$ is not co-periodic. By Lemma 4.14 we have the fixed point $\alpha \in K(\widehat{\Psi}(F))$. Similarly to Lemma 4.13, there are one or two pairs of period two dynamic external rays landing together at α, for which the corresponding dynamic rays for F do not land together. We describe this as an identification made by $\widehat{\Psi}$, and we find other identifications by taking preimages as we did previously in Lemma 4.13. Thus we conclude that the identifications from the lamination of the basilica along the internal rays of every Fatou component of $K(F)$ exist in $K(\widehat{\Psi}(F))$. We want to show that these are the only identifications made by $\widehat{\Psi}$. Since $R_e(t)$ is not co-periodic, neither map $F, \widehat{\Psi}(F)$ is a parabolic map, see [2]. Therefore, the free critical point is in the Julia set for both of these maps. Since each attracting cycle must attract a critical point, and the free critical point is in the Julia set, the maps must each have one attracting cycle, namely that of the marked critical point. It then follows that every bounded Fatou component of F

60

is a preimage of the main disc component, and every Fatou component of $\widehat{\Psi}(F)$ eventually maps to the two cycle of the Fatou components containing the marked critical point and its associated critical value. Therefore, the only identifications made by $\widehat{\Psi}$ are those which come from putting the lamination of the basilica in every disc component of $K(F)$.

2. Now, suppose that $R_e(t)$ is co-periodic. It follows that F and $\widehat{\Psi}(F)$ are parabolic maps, see [2]. We again have the identifications arising from preimages of $\alpha \in K(\widehat{\Psi}(F))$ which are described by putting the lamination of the basilica in each component of $K(F)$. Every other Fatou component of F is then a component of the parabolic basin. In both $K(F)$ and $K(\widehat{\Psi}(F))$, we must have the rays $r_e(t - \frac{1}{3})$ and $r_e(t + \frac{1}{3})$ landing at the parabolic point in the same component of the parabolic basin as the free critical point $-a$. Since $-a$ is the only critical point which could be attracted to the parabolic orbit because of the periodicity of a, this then determines the period of the parabolic point, and we conclude that no further identifications are made, i.e. the rays which land together on the boundary of the parabolic basin in $K(F)$ are exactly those which land together on the boundary of the parabolic basin in $K(\widehat{\Psi}(F))$. $\qquad \square$

We now look to apply this dynamical information to prove our main results in parameter space. We will begin with the easier of our two cases, where we consider a map on the boundary of a type C component of $\mathcal{S}_1$. The following result describes where to find pairs of distinct maps on the boundary of a type C component of $\mathcal{S}_1$ which will be mapped by $\widehat{\Psi}$ to the same image in $\mathcal{S}_2$.

Theorem 4.16. *Suppose $F = \Lambda_i(t)$ on the boundary of a type C component of $\mathcal{S}_1$.*

1. If t is a basilica angle with partner $\tilde{t}$, let $\tilde{F} = \Lambda_i(\tilde{t})$ on the boundary of the same type C component. Then we have $\widehat{\Psi}(F) = \widehat{\Psi}(\tilde{F})$.

2. If t is not a basilica angle, then F is the only preimage under $\widehat{\Psi}$ of $\widehat{\Psi}(F)$.

Proof. Let F be on the boundary of a type C component of $\mathcal{S}_1$ at internal angle t. Suppose there are n external parameter rays landing at F, with arguments $\{t_1, t_2, ..., t_n\}$. Then in the dynamical plane, the n external rays of arguments $\{t_1, ...t_n\}$ all land at the cocritical point $2a_F$. The point $2a_F$ is on the boundary of a Fatou component of F, and the argument of the internal ray in this Fatou component landing at this point is t. Now, for $G := \widehat{\Psi}(F) \in \mathcal{S}_2$, we still have the n external rays of arguments $\{t_1, ..., t_n\}$ landing at the cocritical point $2a_G$ since Ψ preserves arguments of parameter rays, and by Lemma 4.3, $\widehat{\Psi}$ sends the landing point of the parameter ray of argument t in $\mathcal{S}_1$ to the landing point of the parameter ray of argument t in $\mathcal{S}_2$. If t is not a basilica angle, then it follows from Theorem 4.15 that these are the only external arguments for rays landing at $2a_G$. Therefore, we conclude that these are the only arguments for parameter rays landing at G, and $\widehat{\Psi}^{-1}(G) = \{F\}$. However, if t is a basilica angle with partner $\tilde{t}$, then by Theorem 4.15 the arguments of the external rays for F landing on the component whose boundary contains $2a_F$ at internal argument $\tilde{t}$ will be arguments of external rays for G which also land at $2a_G$. This means that G is the landing point of parameter rays of arguments t and $\tilde{t}$ in $\mathcal{S}_2$. We may then conclude that $\widehat{\Psi}^{-1}(\widehat{\Psi}(F)) = \{F, \tilde{F}\}$. $\qquad \square$

We will now focus on the principal hyperbolic component $\widehat{\mathcal{H}}_0$ in $\mathcal{S}_1$, or in other words, the unique type A component. This case is more difficult due to the double cover of internal arguments in this component. It will be convenient to split this component up into four quadrants, which will be separated by the four internal rays of arguments $\frac{1}{3}$ and $\frac{2}{3}$. We will label them so that the first quadrant contains on its boundary the landing map of the external ray of argument zero, and the rest will be labeled in the counterclockwise direction as usual, see Figure 30. We will refer to Quadrants I and III, and similarly II and IV, as opposite quadrants. We

will use these quadrants to give a useful notation for internal rays in $\widehat{\mathcal{H}}_0$. By $R_i^{\mathrm{I}}(t)$, we will mean the internal ray of argument t which lies in quadrant I. Note that we need to be sure that $t \in (\frac{1}{3}, \frac{2}{3})$ for $R_i^{\mathrm{I}}(t)$ to exist. We will take care of the internal rays which bound the quadrants by choosing the odd numbered quadrant which it bounds, i.e. $R_i^{\mathrm{I}}(\frac{1}{3}), R_i^{\mathrm{I}}(\frac{2}{3}), R_i^{\mathrm{III}}(\frac{1}{3})$, and $R_i^{\mathrm{III}}(\frac{2}{3})$ will denote these four internal rays in $\widehat{\mathcal{H}}_0$.

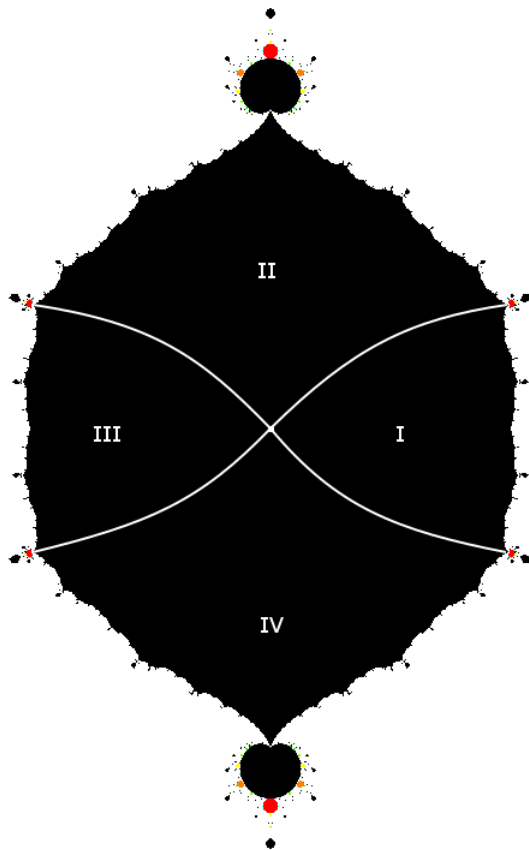Figure 30. The principal hyperbolic component of $\mathcal{S}_1$ split up into four quadrants.

Recall that $\widehat{\Lambda}_i(t)$ denotes the two element set containing the landing maps of both of the internal rays in $\widehat{\mathcal{H}}_0$ of argument t. The following result describes which maps on $\partial\widehat{\mathcal{H}}_0$ which are not landing points of a ray of argument $\frac{1}{3}$ or $\frac{2}{3}$ will share

a common image under $\widehat{\Psi}$ with another map from $\partial\widehat{\mathcal{H}}_0$.

Lemma 4.17. *Suppose $t \notin \{\frac{1}{3}, \frac{2}{3}\}$, and let $F \in \widehat{\Lambda}_i(t) \subset \partial\widehat{\mathcal{H}}_0$.*

1. If t is a basilica angle with partner $\tilde{t}$, then there is one map from $\widehat{\Lambda}_i(\tilde{t})$ in the same quadrant of $\widehat{\mathcal{H}}_0$ as F, and one in the opposite quadrant. For at least one of these maps $\tilde{F} \in \widehat{\Lambda}_i(\tilde{t})$, we have $\widehat{\Psi}(\tilde{F}) = \widehat{\Psi}(F)$.

2. If t is not a basilica angle. Then F is the only preimage of $\widehat{\Psi}(F)$.

Proof. Suppose $t \notin \{\frac{1}{3}, \frac{2}{3}\}$ and $F \in \widehat{\Lambda}_i(t) \subset \partial\widehat{\mathcal{H}}_0$. First, let t be a basilica angle with partner $\tilde{t}$. Since identifications in the lamination of the basilica do not cross the minor leaf connecting $\frac{1}{3}$ and $\frac{2}{3}$, together with the fact that opposite quadrants contain rays of the same range of arguments, we conclude that there is one map from $\widehat{\Lambda}_i(\tilde{t})$ in the same quadrant of $\widehat{\mathcal{H}}_0$ as F, and one in the opposite quadrant. The existence of an identification in the case of a basilica angle, as well as the non existence otherwise, follow similarly to the proof of Theorem 4.16. $\qquad\square$

We conclude this work with the final results. Theorem 4.18 will establish precisely which identifications are made on the boundary of $\widehat{\mathcal{H}}_0 \subset \mathcal{S}_1$ by the map $\widehat{\Psi}$. Taking Theorem 4.18 together with Lemma 4.17, we establish for the unique type A component $\widehat{\mathcal{H}}_0$ what Theorem 4.16 established for each type C component of $\mathcal{S}_1$, with the exception of the four parabolic maps on this boundary which are landing points of co-period two external parameter rays. These parabolic maps are taken care of in Theorem 4.19.

Theorem 4.18. *Suppose $t \notin \{\frac{1}{3}, \frac{2}{3}\}$ is a basilica angle with partner $\tilde{t}$, let $F \in \widehat{\Lambda}_i(t)$, and write $\widehat{\Lambda}_i(\tilde{t}) = \{\tilde{F}_s, \tilde{F}_o\}$ where $\tilde{F}_s$ is in the same quadrant as F, and $\tilde{F}_o$ is in the opposite quadrant. Then $\widehat{\Psi}^{-1}(\widehat{\Psi}(F)) = \{F, \tilde{F}_s\}$.*

Proof. For a contradiction, suppose that $F \in \widehat{\Lambda}_i(t)$ where $t \notin \{\frac{1}{3}, \frac{2}{3}\}$ is a basilica angle with partner $\tilde{t}$, and that $\widehat{\Psi}^{-1}(\widehat{\Psi}(F)) = \{F, \tilde{F}_o\}$. Note that by Lemma 4.17,

only the two cases $\widehat{\Psi}^{-1}(\widehat{\Psi}(F)) = \{F, \tilde{F}_s\}$ or $\widehat{\Psi}^{-1}(\widehat{\Psi}(F)) = \{F, \tilde{F}_o\}$ are possible. First, assume that F is on the boundary of quadrant I in $\mathcal{S}_1$. It then follows that the argument s of the external parameter ray landing at F is in $\left(\frac{23}{24}, \frac{1}{24}\right)$, and the argument $\tilde{s}$ of the external parameter ray landing at $\tilde{F}_o$ is in $\left(\frac{11}{24}, \frac{13}{24}\right)$. Now, define $G := \widehat{\Psi}(F) = \widehat{\Psi}(\tilde{F}_o) \in \mathcal{S}_2$. Then we know that $\lambda_e(\frac{2}{8}) = \lambda_e(\frac{6}{8}) = \alpha_G \in K(G)$, see Figure 26. However, we must also have $\lambda_e(s) = \lambda_e(\tilde{s}) = 2a_G \in K(G)$. This is a contradiction, since the crossing of rays would violate the injectivity of the Böttcher coordinate. Therefore, we have $\widehat{\Psi}^{-1}(\widehat{\Psi}(F)) = \{F, \tilde{F}_s\}$, as desired. The remaining cases follow similarly, with $\lambda_e(\frac{5}{8}) = \lambda_e(\frac{7}{8}) = \alpha_G \in K(G)$ when F is assumed in quadrant II, and $\lambda_e(\frac{1}{8}) = \lambda_e(\frac{3}{8}) = \alpha_G \in K(G)$ when F is assumed in quadrant IV. $\qquad\square$
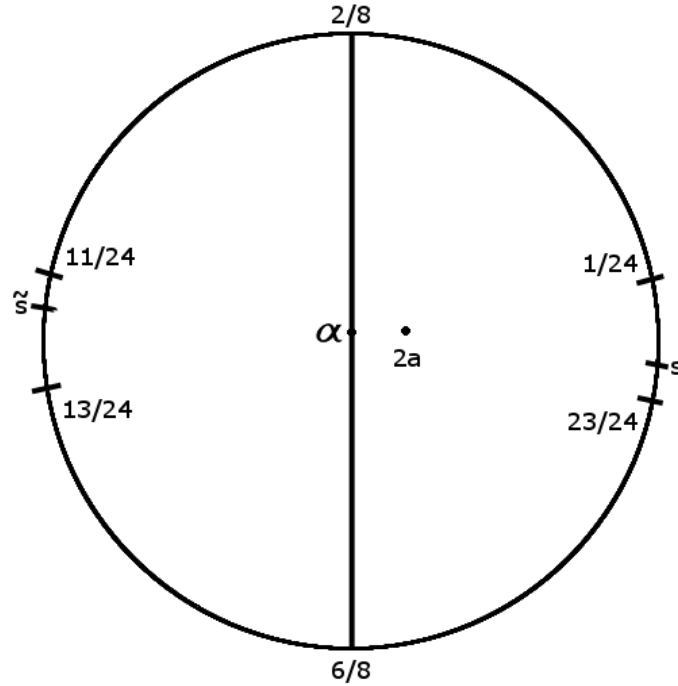

Figure 31. An illustration of the contradiction from the proof of Theorem 4.18 when F is taken in the boundary of quadrant I of $\widehat{\mathcal{H}}_0$.

Theorem 4.19. *Suppose $t \in \{\frac{1}{3}, \frac{2}{3}\}$, and let $F \in \widehat{\Lambda}_i(t) \subset \partial\widehat{\mathcal{H}}_0$, then F is a parabolic map for which $\widehat{\Psi}^{-1}(\widehat{\Psi}(F)) = \{F\}$.*

Proof. The four landing points of internal rays of $\widehat{\mathcal{H}}_0$ of arguments $\frac{1}{3}$ and $\frac{2}{3}$ are landing points of co-periodic external rays of co-period two. From [2], we know that such landing points are necessarily parabolic maps. Since $\widehat{\Psi}$ sends the landing point of the parameter ray of argument t in $\mathcal{S}_1$ to the landing point of the parameter ray of argument t in $\mathcal{S}_2$ by Lemma 4.3, it follows that these four distinct parabolic maps correspond bijectively under $\widehat{\Psi}$ with the four distinct parabolic maps in $\mathcal{S}_2$ on the boundaries of both escape regions which are the landing points of the corresponding co-periodic rays of co-period two. $\qquad\square$

List of References

[1] J. Milnor, "Cubic polynomial maps with periodic critical orbit, Part I," in *Complex Dynamics Families and Friends*, 2009, pp. 333–411.

[2] A. Bonifant and J. Milnor, "Cubic polynomial maps with periodic critical orbit, Part III," 2010, manuscript.

APPENDIX

Table of Notation

$\widehat{\mathbb{C}}$ The Riemann sphere $\mathbb{C} \cup \{\infty\}$.

$\mathcal{S}_n$ The set of all cubic polynomials with a marked critical point having period exactly n.

$\mathcal{C}(\mathcal{S}_n)$ The connectedness locus in $\mathcal{S}_n$.

$\mathcal{E}(\mathcal{S}_n)$ The escape locus in $\mathcal{S}_n$.

$\mathcal{E}_1$ The unique escape region in $\mathcal{S}_1$.

$\mathcal{E}_2^B$ The basilica escape region in $\mathcal{S}_2$.

$\widehat{\mathcal{H}}_0$ The unique hyperbolic component of type A in $\mathcal{S}_1$.

$\mathcal{A}_z$ The basin of attraction of the point z.

$\widehat{\mathcal{A}}_z$ The immediate basin of attraction of the point z.

$K(p)$ The filled Julia set of the polynomial p.

$J(p)$ The Julia set of the polynomial p.

$r_i(t)$ The internal dynamic ray of argument t.

$\lambda_i(t)$ The landing point of the ray $r_i(t)$.

$r_e(t)$ The external dynamic ray of argument t.

$\lambda_e(t)$ The landing point of the ray $r_e(t)$.

$R_i(t)$	The internal parameter ray of argument t.
$\Lambda_i(t)$	The landing point of the ray $R_i(t)$.
$\widehat{\Lambda}_i(t)$	The set of landing points of the two rays $R_i(t) \in \widehat{\mathcal{H}}_0$.
$R_e(t)$	The external parameter ray of argument t.
$\Lambda_e(t)$	The landing point of the ray $R_e(t)$.
Ψ	A conformal isomorphism mapping $\mathcal{E}_1$ to $\mathcal{E}_2^B$.
$\widetilde{\Psi}$	The continuous extension of Ψ to part of $\partial\mathcal{E}_1$.
$\widehat{\widetilde{\Psi}}$	The restriction of $\widetilde{\Psi}$ to part of $\partial\mathcal{E}_1$.

BIBLIOGRAPHY

Ahlfors, L., *Lectures on Quasiconformal Mappings.* Belmont, CA: Wadsworth, 1987.

Bonifant, A., Kiwi, J., and Milnor, J., "Cubic polynomial maps with periodic critical orbit, Part II," *Conform. Geom. Dyn.*, vol. 14, pp. 68–112, 2010.

Bonifant, A. and Milnor, J., "Cubic polynomial maps with periodic critical orbit, Part III," 2010, manuscript.

Branner, B. and Hubbard, J. H., "The iteration of cubic polynomials Part I: The global topology of parameter space," *Acta Math.*, vol. 160, pp. 143–206, 1988.

Branner, B. and Hubbard, J. H., "The iteration of cubic polynomials Part II: Patterns and parapatterns," *Acta Math.*, vol. 169, pp. 229–325, 1992.

Douady, A. and Hubbard, J. H., "The Orsay notes," Available at www.picard. ups-tlse.fr/~buff/OrsayNotes/OrsayNotes.pdf.

Douady, A. and Hubbard, J. H., "On the dynamics of polynomial-like mappings," *Ann. Sci. Ec. Norm. Sup.*, vol. 18, pp. 287–343, 1985.

Faught, D., "Local connectivity in a family of cubic polynomials," Ph.D. dissertation, Cornell University, 1992.

L. Tan, "Branched coverings and cubic Newton maps," *Fund. Math.*, vol. 154, pp. 207–226, 1997.

Milnor, J., "Periodic orbits, external rays, and the Mandelbrot set," in *Géometrie Complexe et Systémes Dynamiques*, 2000, pp. 277–333.

Milnor, J., *Dynamics in One Complex Variable.* Princeton, New Jersey, United States of America: Princeton University Press, 2006.

Milnor, J., "Cubic polynomial maps with periodic critical orbit, Part I," in *Complex Dynamics Families and Friends*, 2009, pp. 333–411.

Rees, M., "Components of degree two hyperbolic rational maps," *Invent. Math.*, vol. 100, pp. 357–382, 1990.

Roesch, P., "Hyperbolic components of polynomials with a fixed critical point of maximal order," *Ann. Sci. Ec. Norm. Sup.*, vol. 40, pp. 901–949, 2007.

Sullivan, D., "Quasiconformal homeomorphisms and dynamics I: Solution of the Fatou-Julia problem on wandering domains," *Ann. Math.*, vol. 122, pp. 401–418, 1985.

Thurston, W. P., "On the geometry and dynamics of iterated rational maps, with appendix by D. Schleicher," in *Complex Dynamics Families and Friends*, 2009, pp. 3–137.